Impact on composite structures

G. A. O. Davies and R. Olsson
Department of Aeronautics,
Imperial College,
London, UK

NOMENCLATURE

BVID	barely visible impact damage
CAI	compression after impact (strength)
CDM	computational damage mechanics
CFD	computational fluid dynamics
C_z	velocity of sound in 'z' (through thickness) direction
d	sandwich core crush diameter
D, D_x, D_y	plate flexural rigidities in (in x and y directions)
F	impact induced contact force
F_{dn}	critical force causing 'n' delaminations
FE	finite element (method)
G_{IC}, G_{IIC}	mode I (peel) and mode II (shear) fracture toughness
h	plate thickness
$m = \rho h$	plate mass per unit area
M_p	mass of projectile or impactor
M_p^*	effective plate mass
q	power of indentation in force/indentation law
$\mathbf{r}$, $\dot{\mathbf{r}}$, $\ddot{\mathbf{r}}$	vectors of structural displacements, velocities, and accelerations
SERR	strain energy release rate
SPH	smoothed particle hydrodynamics
t	time
V_O	impactor velocity.
V_{50}	ballistic limit. (velocity for which 50% or more tests do not penetrate.)
V_r	residual velocity of projectile after penetration
α	indentation of impacted surface
ε_x, ε_y	direct strains in x and y directions
ρ	material density
τ	shear stress

1.0 INTRODUCTION

The problem of impact damage in laminated composite structures, and the consequent reduction in residual strength, has been a topic of continual research for over two decades. The number of journal papers on the subject now runs into four figures and most have been conscientiously reviewed by Abrate(1991, 1994, 1998). This review is not intended to be in the academic tradition, with emphasis on acknowledging the authorship of all the various research initiatives. Instead we present our opinions so that the reader can appreciate our current understanding of the problem, our capability of predicting by analysis, and the scope of the design tools for avoiding structural damage, or at least designing damage tolerant aerospace structures.

There are two types of impact, namely that when a foreign body strikes a structure, or in contrast that when a complete aircraft or helicopter suffers a crash landing of some sort. This latter case is usually discussed as 'crashworthiness' and has become a routine feature of automobile design where the energy-absorbing properties of ductile metals are exploited to the full. The objective here is to design a structure which can deform and absorb energy but leave the passenger compartment more or less intact.

The first case of foreign body impact may span several orders of magnitude in impact velocity, with very different structural consequences.

Dropped tools during manufacture or in service are relatively low velocity events in the range 4-8ms^{-1} with energies up to 50J. Impact due to runway debris at velocities up to 70ms^{-1} can be classified as intermediate velocity with again energies of about 50J. These low velocity impacts can be the most serious in nature for carbon/epoxy composites which have no elasto-plastic energy-absorbing mechanism, with consequently no clear visual evidence of permanent indentation. It is quite possible for a composite structure to suffer fibre damage and massive delamination between plies, but to recover after the impact with very little evidence of the event.

Paper No. 2909. Manuscript received 19 August 2004, accepted 27 August 2004.
The latest in an occasional series of survey papers by leaders in their field.

https://doi.org/10.1017/S0001924000000385 Published online by Cambridge University Press

Barely visible impact damage (BVID) is a hidden menace and the residual strength in compression may be only 30% of the undamaged value.

Ballistic impact due to ordnance or missile fragments can be classified as 'high velocity' in the range 300 to 2,500ms^{-1}. The projectiles may have a mass of only a few grams but their kinetic energy is now 10 to 20kJ. At these speeds the impact event will be so short that the structure may have no time to respond in global flexural or shear modes, and the main issue will be whether complete penetration occurs. Body armour, using various composite materials for example, can be designed to resist penetration.

Finally the term 'hyper-velocity' has come to be applied to satellites and spacecraft which may be struck by micrometeorites at velocities of order 30-70kms^{-1}! Here the impact duration is measured in nanoseconds, conventional heat transport is impossible and both the meteorite (silicon) and impacted structure will vaporise.(Andersen 2001, 2003) Indeed the aim of protective shields is to encourage this so that only a gaseous cloud hits the payload.

For all forms of impact the structural designer must evaluate the threat and ensure that the structure can cope. This means that some analysis of the event must be undertaken. In this review we cover experimental studies to establish the nature of the impact damage for various structural types. 'Theoretical' analysis follows where we use the term for simple, often closed form, solutions where possible. This enables the designer more easily to understand the effects of the main variables such as the mass of the impactor, the mass and stiffness of the impacted structure and its geometry. Numerical simulation is next described with as many variables as possible in this limited review. Commercial computational codes for simulating impact, and the loading of the damaged structure, have become more user-friendly and less costly to use. A computational model frees the user from the need to approximate the global and local geometry, the material's constitutive laws, and allows the user to simulate a strength test of the damaged structure after the impact event.

Finally a brief mention is made of impact-resistant and crashworthy composite structures to show that ductile materials can actually be out-performed.

2.0 EXPERIMENTAL STUDIES OF THE EFFECT OF IMPACT

Extensive reviews of impact experiments and strength after impact tests have been provided by Abrate(1991, 1994, 1997) and Richardson and Wisheart(1996). A detailed review of more than 30 experimental studies by a single research group was provided by Olsson(1999).

2.1 Indentation response

Impact on composite laminates typically results in concentrated contact loads, which cause local indentation in addition to any deflection of the laminate. Indentation of sandwich panels involves both an indentation and a local deflection of the loaded face sheet. Thus the measured impactor displacement will generally be *larger* than the actual deflection of the laminate. A low contact stiffness will, obviously, reduce the total structural stiffness and the peak impact load. Impact loads met in practice typically result in indentation of a few tenths of a millimetre for monolithic laminates and several millimetres in sandwich panels. Thus, indentation of monolithic laminates is insignificant for impacts causing deflections of several millimetres, which is typical for large mass impact on thin laminates. However, indentation has to be considered for sandwich panels and is important for thick laminates, or small-mass high-velocity impact which results only in local deflection of the laminate.

Indentation tests are either performed on panels placed on a flat rigid support, or by measuring differences between front and back face deflections on panels with an unsupported back face. The latter method is more representative for impact on flexible targets and was used by Tan and Sun(1985) and by Wu and Shyu(1993) to study indentation of carbon/epoxy laminates. These studies reveal that the load-indentation at low loads is in good agreement with the 1·5 power law predicted by Hertzian contact theory. At higher loads matrix cracking and delamination causes a decreasing indentation as the reduced flexural stiffness results in a redistribution of the contact pressure to a larger area. This effect, termed 'wrapping' has also been theoretically predicted for large deflection of undamaged laminates. Indentation tests on laminates resting on a rigid foundation agree with Hertzian contact theory for moderate loads, while loads of more than 10-20kN result in softening caused by fibre damage, Swanson and Rezae(1990). In addition, there is a stiffening finite thickness effect, which clearly depends on the ratio between the indentation depth and laminate thickness. A discussion of these counteracting effects was provided by Christoforou(1993).

Experimental studies of the indentation of sandwich panels with different material systems have been reviewed by Olsson and McManus(1996) and Olsson(2002). Comparisons of the static and dynamic indentation of sandwich panels were provided by Rinaird(1995) and Mines, Worrall and Gibson(1990). The load-indentation relation of sandwich panels is usually dominated by local face sheet deflection and is fairly linear up to face sheet penetration, which has been shown to be a combined effect of early core crushing and face sheet membrane effects, Olsson and McManus(1996).

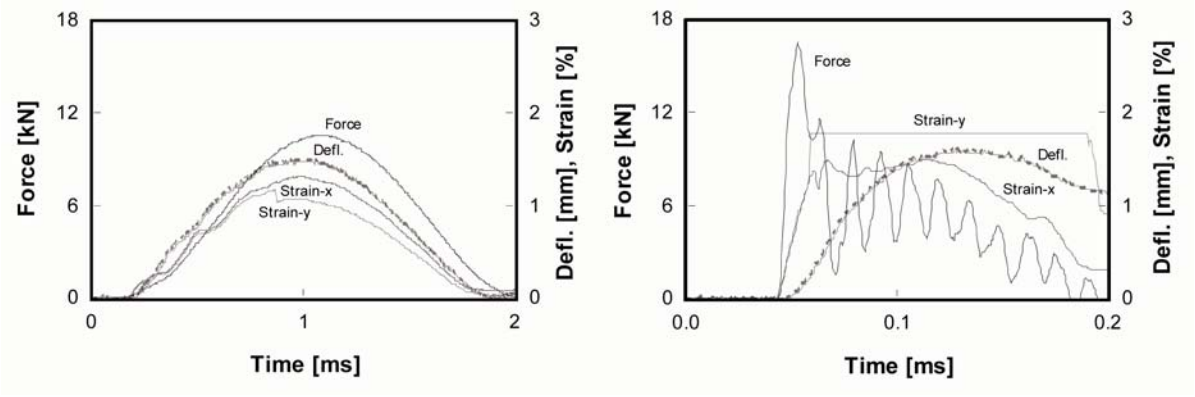
In summary, indentation of thin laminates is only of importance at low loads, where the Hertzian contact theory is sufficient. At higher loads the theory becomes increasingly inaccurate but this has a small influence on the response, which is then dominated by laminate deflections. Thick laminates obey the Hertzian contact theory up to fairly high loads, where softening due to fibre damage occurs. Indentation of sandwich panels is usually significant and involves core crushing and large face sheet deflections, which result in a fairly linear load-indentation relation.

2.2 Low to medium velocity impact response

Small mass impactors with moderate velocity cause an entirely different response than large mass impactors with a low velocity. This is illustrated by Fig. 1 which shows the response and damage of a clamped 125 × 125 × 6mm flat laminate impacted at 10J with a small and large mass impactor. The selected impact energy was just above the delamination threshold value for large mass impact on this specific geometry. It is noted that the load, deflection and strains essentially are in phase for the large mass impact, while the corresponding quantities for the small mass impactor are out of phase. Furthermore, the small mass impactor results in a higher peak load and larger delaminations. The reason for this difference is that impact by small masses is associated with short impact times, which results in a wave controlled local response of the laminate. This phenomenon has been studied with optical methods by Fällström *et al*(1989).

Impact by large masses results in more or less bell-shaped load and deflection histories as long as the laminate remains undamaged. Membrane effects caused by large deflections result in a more 'pointed' load history, while fibre fracture results in a 'capped' load curve, as illustrated by Fig. 18. Delamination onset is easily detected as a sharp load drop, followed by violent oscillations, Fig. 2, as demonstrated by extensive experimental data presented by Schoeppner and Abrate(2000) and Cartié and Irving(2002). This effect is often hidden by excessive filtering of the load signal, which may also cause a phase lag between the load and deflection histories, as illustrated by the large mass impact case in Fig. 1(a). The delamination threshold load theoretically predicted by Davies and Robinson(1992) has been validated by numerous experimental studies, e.g. Davies *et al*(1994), Olsson *et al*(2000) and Cartié and

https://doi.org/10.1017/S0001924000000385 Published online by Cambridge University Press



(a) 1·5kg impactor (b) 10g impactor

Damage



Figure 1. Response and delaminations due to 10J impact by a large and small mass impactor.

Irving(2002). Low-velocity large-mass impact allows the laminate to deform in an essentially static mode. As a result, impact tests and static tests result in similar load-deflection curves. Interpretation of quasi-static large-mass impact response is often facilitated by plotting the load-deflection trace, which simplifies identification of membrane effects and onset of delamination and fibre damage, Fig. 2. It also delivers the total energy absorbed during the impact event. The similarity between large mass impact and static loading has been illustrated by Elber(1983) and Kaczmarek and Maison(1994) for monolithic laminates and by Lagace *et al*(1993), Rinaird(1995) and Ferri and Sankar(1997) for sandwich panels.

Experimental studies of large-mass impact and damage formation in laminated cylinders by Christoforou, Swanson and Beckwith(1989), Wardle and Lagace(1998) and Curtis *et al*(2000) demonstrate the similarities between large-mass impact response and static loading. Load histories are often similar to flat plates, although Wardle and Lagace(1998) observed a specific response feature of convex panels where snap-through at a certain load caused a

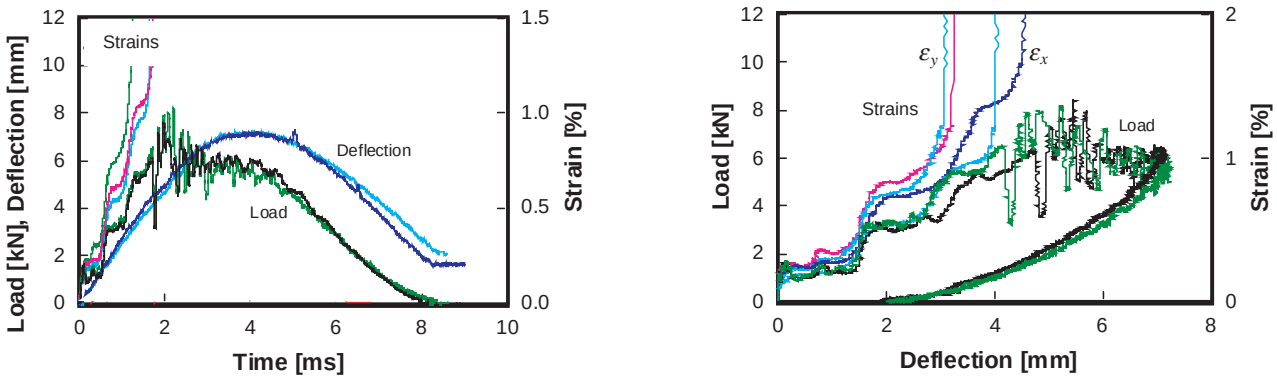


Figure 2. Response during 30J large mass impact on two 4·2mm laminates.

https://doi.org/10.1017/S0001924000000385 Published online by Cambridge University Press

significant stiffness loss.(see also Figs 23 and 24). The impact response of stiffened panels is similar to that of simple laminates, although the number of published studies is fairly limited, Dost *et al*(1993), Bishop *et al*(1994) and Wiggenraad, Zhang and Davies (1999). Thus a bell shaped load history is retained for large mass impacts, while the wave controlled local response is retained for small mass impacts far from stiffeners. The loads and deflections during large mass impacts are, however, influenced by the stiffness of the compound skin-stiffener structure. For impacts close to stiffeners the impact response may differ considerably from the impact on plain laminates. The delamination threshold load (Equation (6)),derived for simple laminates, has also been found valid for stiffened panels, Wiggenraad, Zhang and Davies(1999).

Quasi-static impact response is typical for impactor masses significantly larger than the impacted laminate. A decreasing impactor mass causes superimposed higher frequency load oscillations of increasing amplitude until the response at some point becomes localised and entirely governed by wave propagation. This phenomenon is theoretically explained in Section 3 but systematic experimental studies of the transition region seem to be lacking.

2.3 High velocity impact.

The term 'high velocity' can be used to describe a range of values from $70ms^{-1}$ to $70kms^{-1}$, and the consequent structural response and damage will be different at the lower and higher values. We discuss first the effects of 'ballistic' impact up to $2{,}000ms^{-1}$ and then 'hypervelocity' for impacts in space at much higher closing velocities.

Firstly, unlike the low velocity response, the transverse dilatational waves shown in Fig.11a can cause initial damage since the strains are of order V_o/C_Z (Equation 4) and, for a matrix speed of sound of $2{,}000ms^{-1}$, a velocity of even $70ms^{-1}$ will induce compressive strains of order 3% even before any further flexural response. Another factor at these higher velocities is that the almost instant structural surface velocity will induce high inertial resistance and a high impact force from the projectile. This will cause a 'shear-out' plug unless the composite structure is more than (say) a centimetre thick. The impact event is short and no global structural modes are excited at all. The induced stress field before perforation is highly local, may be three dimensional, and strain rates may be of order 10^2S^{-1} even for velocities as low as $70ms^{-1}$. The material properties for glass and aramids will change at these values but carbon will not until 10^3S^{-1}. The onset of perforation will also depend on the projectile nose shape although this influence is small for ordnance (300-$600ms^{-1}$) and for missile fragments (up to $2000ms^{-1}$)

Because penetration is likely for ordnance, many of the experimental studies have centred on achieving no penetration at all. This 'ballistic limit' is usually termed V_{50} implying a value at which at least 50% of tests will not perforate. With this aim a large number of tests have been published and discussed by Cantwell and Morton(1989, 1991). It is possible to find out experimentally the effect on the energy absorbed, or the ballistic limit, of target thickness, fibre surface treatment, interlaminar toughness, and so on, but the answers will depend on the particular composite chosen and qualitatively may be obvious anyway. For example Roylance(1980) showed that raising the specific fibre stiffness increased the in-plane velocity of sound and hence more of the plate is affected during the event. A large number of experimental studies have been undertaken on the design of body armour to raise the ballistic limit. This usually involves a hard brittle layer (say of ceramic) which will flatten and decelerate a metal projectile but then rely on a flexible backing plate to absorb the remaining energy, mostly by large-deflection membrane stresses.

There are two cases where local penetration by a high velocity projectile may not be the sole issue. 'Soft body' impact such as bird strike is one. Here the impactor will suffer gross distortion over a longer timescale (millisecs) so the structure will experience a distributed pressure and possibly significant gross structural deformations.

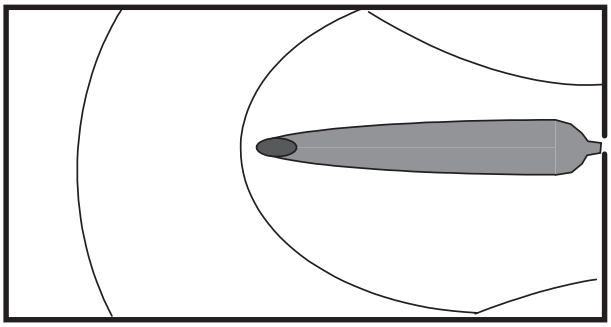


Figure. 3. Hydraulic shock pressure waves and trailing cavity wake.

For bird strike an international standard jelly-like cylinder has been agreed for demonstration and certification purposes, and tests on leading edges and engine fans are obligatory. The effect on high speed engine fans is potentially serious since even a modest permanent deformation can cause very large out-of-balance forces leading to destruction.

The other case is that of hydraulic shock (or ram) when a missile fragment strikes a wing box containing fuel. A fragment of 5-10g and velocity of $2{,}000ms^{-1}$ has an energy of 20kJ and will easily perforate a composite skin of 5-10mm thickness, suffering some flattening in the process. However on entering the fluid it will decelerate to a standstill in roughly 30-40 projectile diameters. The absorbed energy is converted to pressure waves which will affect even remote corners of the wing-box. A compressive wave is generated ahead of the projectile but behind the projectile it trails a cavitation wake since the fluid cannot support tension. Figure 3 indicates this, and the wake shows that the fluid has experienced a significant volumetric strain leading to the very high pressures. Transient pressures of several hundred bars are possible and no structure can withstand this, although the nature and extent of damage will depend on the structural geometry, mass and stiffness. Alleviation is an aim for modern combat aircraft, such as introducing very flexible connections between spars and skins, but no details are in the public domain. A partial alleviation is provided by the structure itself since the outer skins will respond to the high pressures by accelerating away from the driving fluid and causing a cavitation boundary layer. A not dissimilar event was responsible for the recent loss of Concorde on take off. Here a portion of a disintegrated tyre hit the wing 'flat face on' and did not penetrate, but sent a strong compressive wave into the fuel which then reflected and hit the lower wing surface, causing a portion to fracture end eject. (Jupp(2003)).

A quite different situation is that of hypervelocity impact which occurs when satellites meet debris or micrometeorites at velocities in the range 7-$70kms^{-1}$. At these velocities and energies no conventional structure can resist penetration, which could be disastrous for the payload, so the emphasis is on designing a bumper to absorb the energy in nanoseconds. One form consists of a sandwich with an outer thin skin of aluminium which receives the first impact. This is instantaneous with no time for thermal transport so the skin and micrometeorite will vaporise resulting in an expanding pressurised cloud which can impact on the second skin some cms away, and which can absorb the residual energy. At the time of the Giotto satellite, launched to intercept the Halley comet, only a numerical simulation was possible to design a shield,(Laine & Felici(1982)) The interested reader is referred to many articles on this topic edited by Andersen(2001, 2003).

2.4 Impact and indentation damage

Impact damage is caused by the interaction of indentation and global deflection while pure indentation damage in laminates and sandwich

https://doi.org/10.1017/S0001924000000385 Published online by Cambridge University Press

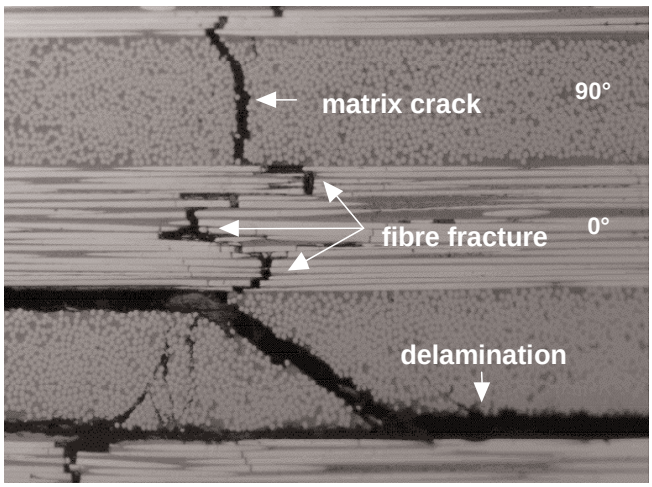


Figure 4. Damage types in impacted fibre reinforced laminates.

panels is observed when the panel back face is supported or when the effect of global deflection is negligible. Indentation damage and impact damage in laminates involves a number of common damage features such as matrix cracks, delaminations and fibre fracture, Fig. 4, although indentation damage is much more localised. Thus, indentation of thick laminates was observed to cause fibre fracture and matrix cracking within a distance of about one contact radius from the loaded surface, Poe(1991). An extensive review of observations of impact damage was given by Hull & Shi(1993). An impact damage may usually be separated into a small local region where damage is induced by stresses resulting from flexure and the contact load, and a surrounding region whereby damage is induced by stresses resulting from flexure and transverse shear forces. For impacts causing large deflections, membrane strains will be significant, particularly close to the impact centre. A local residual deflection is frequently observed, which influences the subsequent compressive behaviour, Melin and Schön(2001). The sequence of damage formation during static point loading and large mass quasi-static impact has been studied in detail by Kaczmarek and Maison(1994).

Matrix cracks caused by tensile, compressive and shear stresses are normally dispersed within the entire damage region with a concentration close to the impact centre.

Delaminations are primarily induced by interlaminar shear stresses, which are enhanced by matrix cracks and ply stiffness mismatch. Fractographical evidence of mode II (shear) dominated delamination growth has been provided by Srinivasan *et al*(1992). A typical distribution of delaminations is shown in Fig. 5. Fractographic studies of the individual delaminations in laminates have been provided e.g. by Levin(1991) and Hull & Shi(1993) for large-mass quasi-static impact and by Kumar & Rai(1993) for small mass dynamic impact. The delaminations are usually 'peanut shaped', extending along the fibres of the lower ply and normally appear between plies of different orientation with an increasing size for increasing misalignment angles. These phenomena have been qualitatively explained by Liu(1988).

A single large delamination frequently appears in the lowermost interface, along matrix tensile cracks induced by bending. However, the separated sublaminate is usually too thin to have a significant influence on post-impact strength and buckling induced delamination growth. The region affected by remaining delaminations is usually barrel shaped in thick laminates and slightly conical, expanding towards the non-impacted face in thin laminates, Fig. 6. Olsson *et al*(2000). This effect may be explained by the influence of membrane stresses on the strain energy release rate through the thickness, Suemasu & Majima(1998).

Local compressive and shear failure of fibres has been observed close the contact area, while local tensile failure of fibres has been observed on the opposite face and in the vicinity of large matrix cracks. More extensive fibre failure normally occurs in the central part of the delaminated region, and appears to be fairly uniformly distributed through the thickness, Sjögren, Krasnikovs and Varna(2001). It was noted that fibre failure in thin laminates generally affects more plies and is more extensive than in thick laminates, indicating the importance of membrane stresses in formation of fibre fracture, Fig. 7.

The fractographic observations discussed so far are based on studies of plain laminates. Fractographic studies of stiffened structures

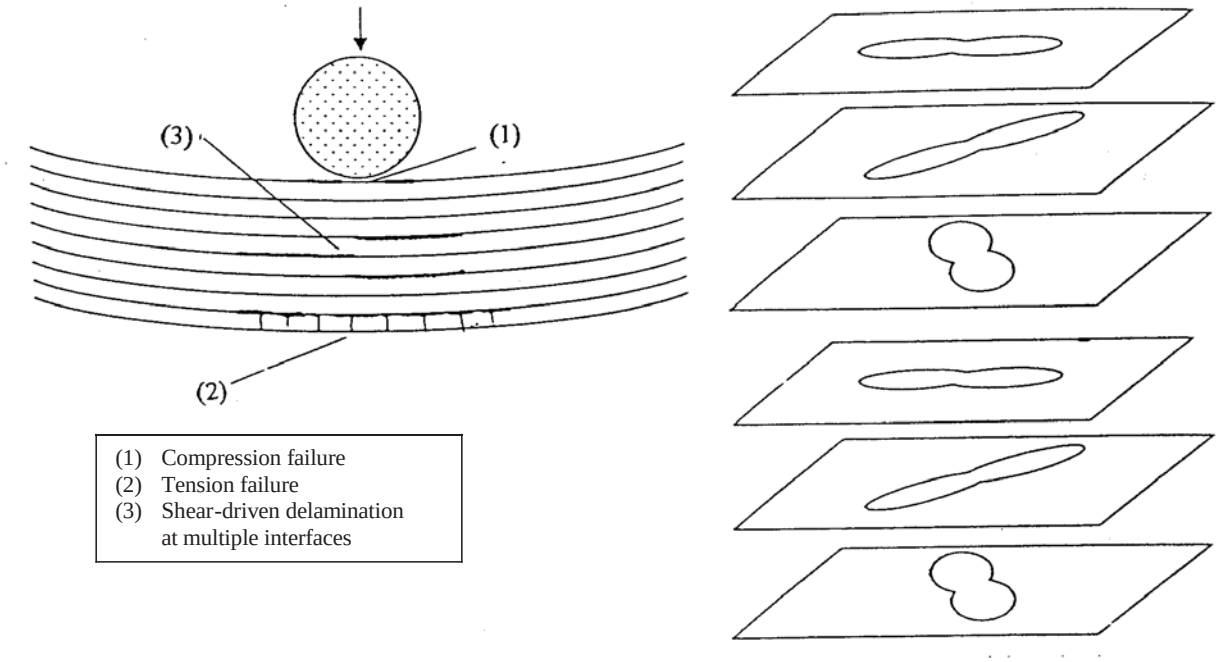


Figure 5. Individual delaminations caused by impact.

https://doi.org/10.1017/S0001924000000385 Published online by Cambridge University Press

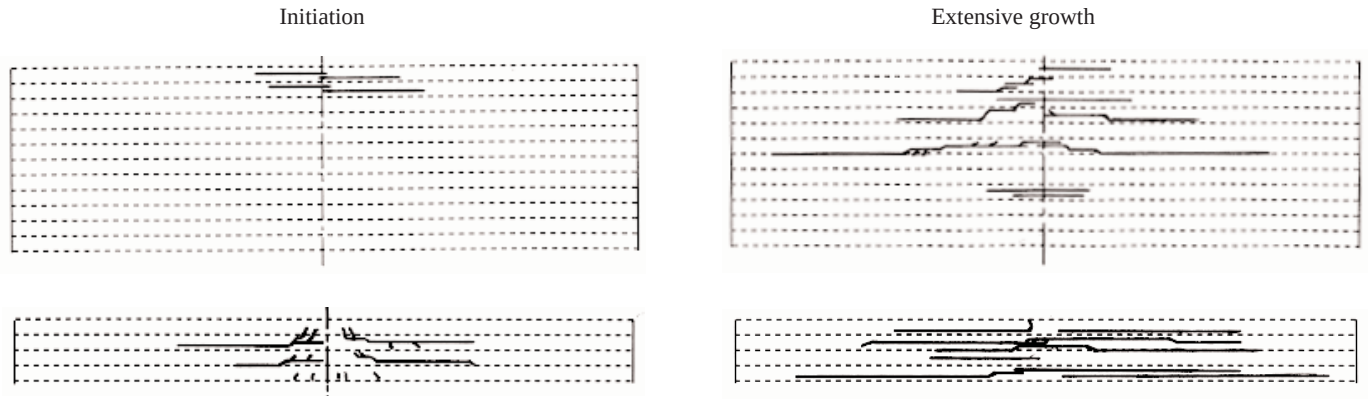


Figure 6. Distribution of delaminations for a 48 ply and 16 ply laminate.

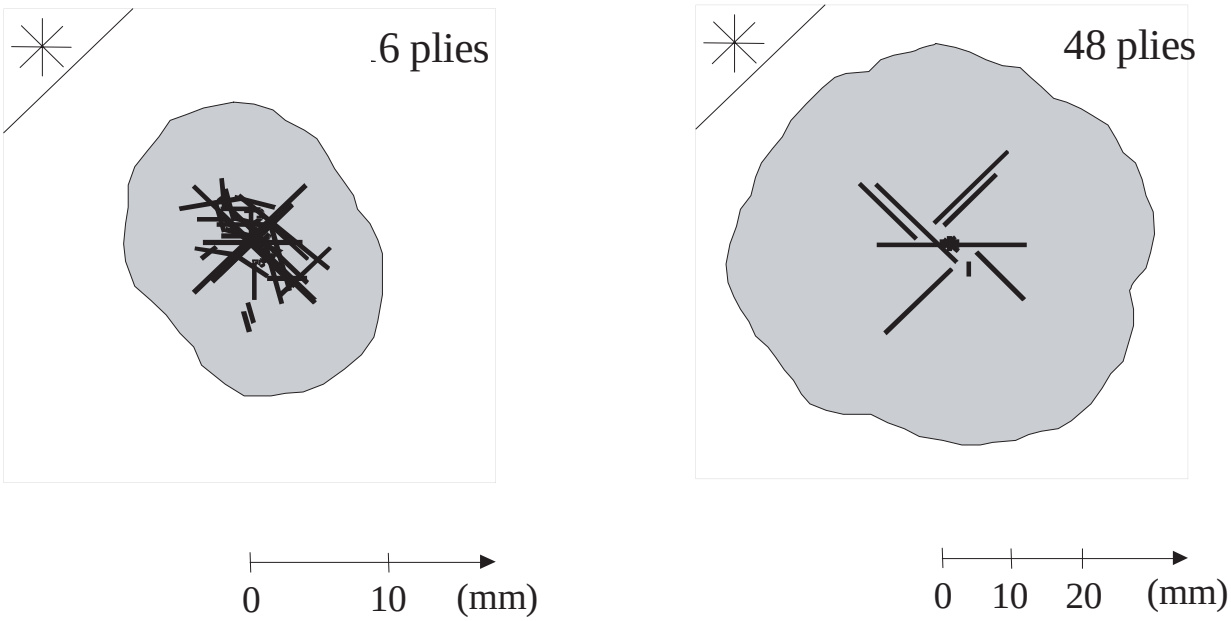


Figure 7. Fibre damage in a 16 ply (left) and 48 ply (right) laminate.

are relatively scarce. A detailed fractographic study of impact damage in skin-stringer CFRP panels was provided by Greenhalgh *et al*(1996). The study included impacts at mid bay, at stringer foot edge, and over stringer centre. Similar studies have also been presented by Wiggenraad, Zhang & Davies(1999) and Wiggenraad, Greenhalgh & Olsson(2002). Impact damage at some distance from stringers is similar to those of plain laminates. Delaminations close to the stringer foot tends to be elongated along the stringer. Impact directly above a stringer initially results in local crushing with extensive fibre failure and small delaminations close to the impacted surface, while higher impact energies result in more distributed delaminations, extending along the skin-stringer interface.

Detailed fractographic studies of sandwich panels have been provided by Williamson & Lagace(1993) for Nomex cores, by Rinaird(1995) for aluminium honeycomb cores and by Shipsha, Hallström & Zenkert(2003) for foam cores. Impact damage in sandwich panels involves core crushing at low impact loads and a more or less evident dent in the face sheet, Fig. 8. Additional damage types include skin-core debonding and core cracking, particularly in foam cores. The damage types in laminated face sheets of sandwich panels are similar to those in monolithic laminates, although delaminations usually are more local, and residual deflections more pronounced. It should be noted that a significant residual deflection of the plies closest to the core may be hidden by surface plies, which have recovered a flat shape after delamination. For face sheets debonding from the crushed core there will be a more or less complete recovery of all the plies, as discussed in Section 4.

2.5 Strength after impact

The tensile and compressive failure mechanisms of impacted composite structures differ considerably with larger reductions in com-

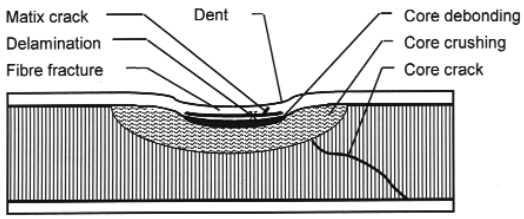


Figure 8. Impact damage features in sandwich panels.

https://doi.org/10.1017/S0001924000000385 Published online by Cambridge University Press

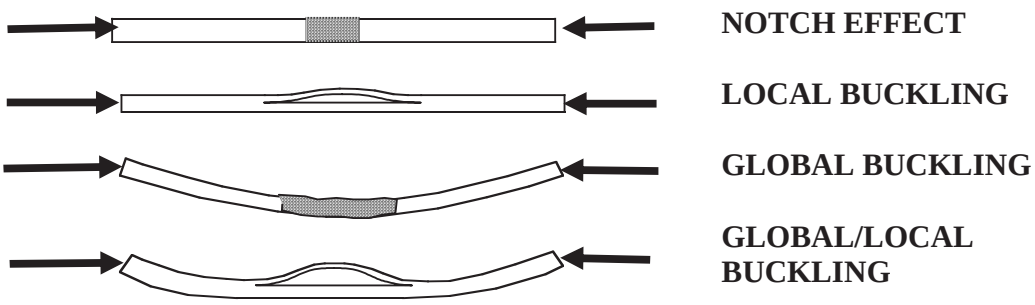


Figure 9. Failure mechanisms in compression after impact.

pressive properties, Abrate(1991). Tensile failure of impacted laminates is primarily governed by fibre fracture, although it may be preceded by matrix cracking and subsequent delamination growth. Premature fibre fracture is caused by stress concentrations due to broken fibres and other damage in the damage zone. Fibre damage can reduce the local tensile stiffness by 80% or more, Elber(1983) and Sjögren, Krasnikovs and Varna(2001), but the reduction in global strength is smaller due to the inherent toughness of the material.

Compressive failure of impacted laminates includes a number of competing and interacting failure mechanisms, i.e. global buckling, local buckling, buckling induced delamination growth and in-plane compressive failure due to stress concentrations, Fig. 9. The reduction in strength can be 70 % or more, Pritchard and Hogg(1990). An additional catastrophic failure mode for stiffened compression panels is stiffener detachment. Premature global buckling may be caused by asymmetries caused by the initial damage, or by local buckling and/or delamination growth during subsequent loading. Local buckling of delaminated sublaminates promotes buckling-induced delamination growth and premature global buckling. Catastrophic in-plane compressive failure normally involves fibre kinking at in-plane stress concentrations caused by impact damage with extensive fibre failure, which can reduce the local compressive stiffness/strength by about 50%, Sjögren, Krasnikovs & Varna(2001). Stiffener detachment normally involves buckling induced unstable delamination growth along the skin-stiffener interface, followed by panel failure as removal of a stiffener usually reduces the buckling load by three quarters.

The strength after impact of plain laminates is covered by literally hundreds of studies, Abrate(1991, 1994). It is worth noting that most compressive coupon tests constrain laminate buckling, either by use of anti-buckling plates or by the sheer choice of dimensions and boundary conditions. Figure. 10 presents the effect of impact damage size on compressive failure strain (for specimens with prevented global buckling) after impact on panels of different configurations and materials, Olsson(1999). Typically the failure strain drops exponentially to a low asymptotic value. The graph shows a moderately increasing strength for tougher resins, when progressing from brittle epoxy (914C) to toughened epoxy (6376) and thermoplastics (PEEK). The figure also illustrates the decrease in strength with increasing amount of fibre fracture, as laminates impacted at larger span/thickness ratios were found to experience more severe fibre fracture. Obviously, results obtained from tests with prevented global buckling are only applicable for structures where in-plane failure or delamination growth do not couple with global skin buckling, or for damage close to stiffeners in post-buckling structures. A method to mimic the

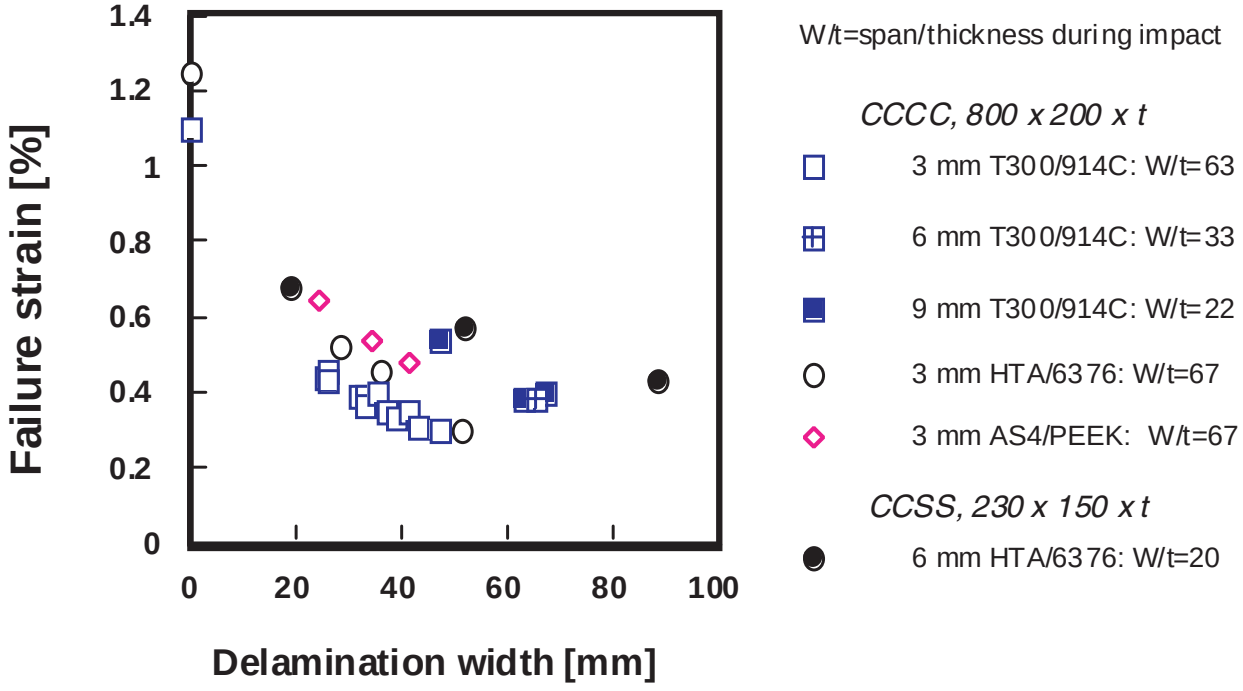


Figure 10. Influence of delamination width on compressive failure strain, Olsson (1999).

https://doi.org/10.1017/S0001924000000385 Published online by Cambridge University Press

influence of stiffeners in compressive tests with plain laminates was suggested by Habib(2001). In contrast, tensile tests on coupons can be expected to be generally relevant for structures, provided a similar damage is present and that the ratio of coupon width to damage width is sufficient to ignore finite width effects.

Experimental studies of the failure mechanisms of stiffened panels have been presented by Wiggenraad, Zhang & Davies(1999), Rosseau, Baker & Hethcock(2000), Kong, Hong & Kim(2000), Wiggenraad, Greenhalgh & Olsson(2002) and Greenhalgh *et al*(2003). Impact damage seems to have a marginal influence on the buckling load of plain laminates with all sides supported, except when significant portions of the width are affected by fibre fracture, Olsson(1999), or when the boundary conditions are relaxed by impact close to edges with strong rotational constraint, Nilsson(1994). Similar conclusions can be drawn from experiments on stiffened panels by Kong, Hong & Kim(2000), Wiggenraad, Greenhalgh & Olsson(2002) and Greenhalgh *et al*(2003). There exists a strong interaction between global skin buckling modes and impact location. Thus impact damage may occasionally cause changes in the global buckling mode, Nilsson(1994) and Wiggenraad, Greenhalgh & Olsson(2002). The latter study also indicated that delamination growth is promoted by location at a skin buckling crest and is retarded by location at a buckling node line, although no systematic experimental study of this phenomenon is known.

Comparisons of the effect of artificial delaminations and impact damage on compressive failure in medium size specimens with local/global buckling have been provided by Davidson(1990) and Asp, Nilsson & Singh(2001). These studies reveal that impacted panels buckle more gradually, without distinct bifurcation loads. The differences may partly be due to a local softening of the impacted material caused by matrix cracking and fibre fracture. A more obvious difference is the significant flatness imperfections observed after impact. This has been observed to cause simultaneous co-directional buckling of all delaminated plies at low loads, Melin & Schön(2001), rather than the sequential symmetric or antisymmetric buckling of perfectly flat sublaminates.

Fractographic studies demonstrate that delamination growth induced by local buckling primarily occurs along interfaces where the fibres of the adjacent ply in the buckling sublaminate coincide with the preferential growth direction, i.e. perpendicular to the applied load. It has been observed that initial delaminations tend to migrate to such preferential interfaces via matrix cracks ('ply jumping'), Greenhalgh & Singh(1999). However, ultrasonic studies prior to final failure have demonstrated much smaller delamination growth for impact damage than for artificial delaminations of equal size, Greenhalgh *et al*(2003). Possible causes may be a smaller in-plane stiffness or thickness of the sublaminates in the actual impact damage, which reduces the available strain energy release rate, or the fact that each individual delamination is smaller than the assumed projection of all delaminations.

Sandwich panels exhibit all the failure modes of monolithic laminates, although global buckling of sandwich panels is unusual due to their larger relative flexural stiffness. In contrast, in-plane notch type of failure is more likely to occur, as laminated skins of sandwich panels usually are thinner and more susceptible to penetration or fibre fracture. The frequent assumption of delamination growth or skin-core separation due to outward skin buckling is not supported by experiments, which usually demonstrate an inward skin buckling initiated by the residual dent present after impact. A resulting specific failure mechanism for sandwich panels is dent growth (or 'dimple propagation') with progressive core crushing. This failure mechanism has been studied experimentally by Tsang and Lagace(1994), Cvitkovich and Jackson(1999) and Davies *et al*(2004a).

Finally the question arises as to whether a panel with an existing applied compression loading, which is then impacted, will fail at a lower applied load than when the impact damage is created before the loading is applied. Some early work by Starnes *et al*(1979) is reported at medium to high velocities. A more recent paper by Zhang *et al*(1999) covers the regime of low velocity damage. Initial preloading will affect a panel in several ways. The applied compression may reduce the stiffness, the consequent impact force, and hence create less damage. However, if the applied strain is near the material's strength then more damage may occur as impact-induced strains occur. These effects depend on panel size, thickness and stiffness, and boundary conditions, but can be quantified by three non-dimensional parameters.

1. The ratio of the applied load to the panel initial buckling load.
2. The ratio of impact energy to that which causes delamination — or even better the ratio of the impact-induced force to the critical value (Equation (6))
3. The ratio of the applied strain to the static compressive failure strain.

In Zhang it was found that the preload failure load was only marginally less than the usual CAI load even when all three parameters were close to unity.

3.0 THEORETICAL MODELS FOR EFFECTS OF IMPACT

3.1 Characteristics of theoretical models

Here we will use the term theoretical models for models based on closed form expressions rather than on use of computational mechanics like finite element or boundary element methods.

The main advantage of theoretical models is the insight provided by closed form expressions, which directly show the influence of different parameters. An additional advantage is the speed in obtaining results, which is suitable in early design stages and for large parametric studies. Their main disadvantage is the limitation to fairly simple geometries and no or limited ability to model damage growth. Thus, with a few exceptions, theoretical methods are suitable for prediction of damage initiation rather than for simulation of the actual growth. By contrast computational mechanics becomes a strategy for more complex geometries and numerical experiments with formation of damage.

Theoretical models may be divided into two main categories: multi-degree-of-freedom models and one- or two-degree-of-freedom models. Multi-degree-of-freedom models are normally based on numerical mode summation which rarely allows explicit expressions for parameter influence. Thus, they may be seen as a quicker and cheaper alternative to other computational methods. One- or two-degree-of-freedom models usually allow closed form solutions which explicitly show the influence of parameters, but have limited flexibility in handling different loading cases and complex geometries.

Theoretical models are normally designed to address either response and damage formation *during* impact or response and damage growth *after* impact (particularly compressive strength after impact. CAI) while many finite element models are able to address both problems with the same model. For this reason theoretical models for impact response and response after impact will be addressed in two separate sections.

3.2 Theoretical models for indentation

All impact response models rely on an appropriate model of the impactor-plate contact. It is important to realise that indentation is superimposed on the structural deflection due to shearing and bending. Thus, changes in the contact behaviour *do not affect* the impact load when the expected indentation is *significantly smaller* than the shear and bending deflections. Contact models may use theoretically or experimentally determined load-indentation relations.

Theoretical models for indentation of monolithic laminates usually rely on generalisations of the classical Hertzian solution for a half-space, where the contact force (F) is related to the indentation (α) by the power law $F = k_\alpha \alpha^{1.5}$. Improved solutions have considered

https://doi.org/10.1017/S0001924000000385 Published online by Cambridge University Press

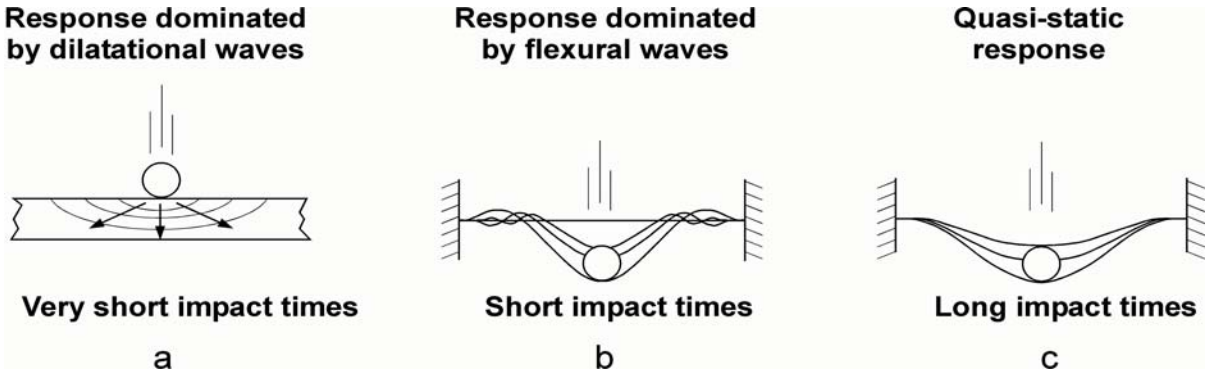


Figure 11. Response types for impacted structures.

orthotropy, Mittal & Khalili(1994), finite thickness and influence of load induced curvature ('wrapping') Sankar(1985), Wu & Yen(1994), Suemasu, Keth & Maier(1994) and inelastic indentation, Cairns(1991) and Christoforou(1993). To capture inelastic unloading and the energy lost in forming irreversible contact damage we need to use a different law for unloading, Tan & Sun(1985). The complications introduced by improved contact models are, however, rarely justified for monolithic laminates, as loads of interest normally cause highly localised contact damage and indentations much smaller than the corresponding deflections.

In contrast, soft core sandwich panels have comparatively low indentation stiffness and high flexural stiffness, so that the indentation often is of the same order as the panel deflection. The indentation of such panels is the sum of local face sheet deflection and true indentation of the face sheet, and commonly involves significant core crushing/yielding and face sheet membrane effects. The resulting load-indentation relation can usually be approximated by a linear relation $F \approx k_\alpha \alpha$. Indentation models for point like loading of sandwich panels with core crushing and face sheet membrane effects were presented by Olsson & McManus(1996) and Türk & Hoo Fatt(1999), where the latter model is limited to purely plastic core behaviour. Expressions to predict initiation and effect of fibre fracture and penetration during sandwich indentation were later provided by Olsson(2002). Line load indentation of sandwich beams was modelled by Soden(1996).

3.3 Theoretical models for impact response until damage initiation

In this section we will discuss the *elastic* response of flat plates, i.e. *up to the point of damage initiation*. Criteria for damage initiation will be discussed in Section 3.4, and the effects on subsequent response in Section 3.5. Before describing available models for impact response it is useful to review different types of elastic impact response for plates, as the response type is crucial for selection of a proper model. An impact initiates elastic waves propagating from the impact point, where the influence of the waves gradually fades away due to material damping and wave scattering. For impact times in the order of the transition time for through-the-thickness waves the response is dominated by three-dimensional wave propagation, Fig. 11(a). For longer impact times flexural waves and shear waves govern the response, Fig. 11(b). For times much longer than the time needed by these waves to reach the plate boundaries the lowest vibration mode of the impactor-plate system predominates, Fig. 11(c). Eventually the deformation mode approaches a purely static deformation.

The impact time under elastic conditions depends on the impactor mass M_p, the plate mass in motion and the structural stiffness. To choose a relevant structural stiffness we must consider the plate region actually affected by the impact. By considering the relation

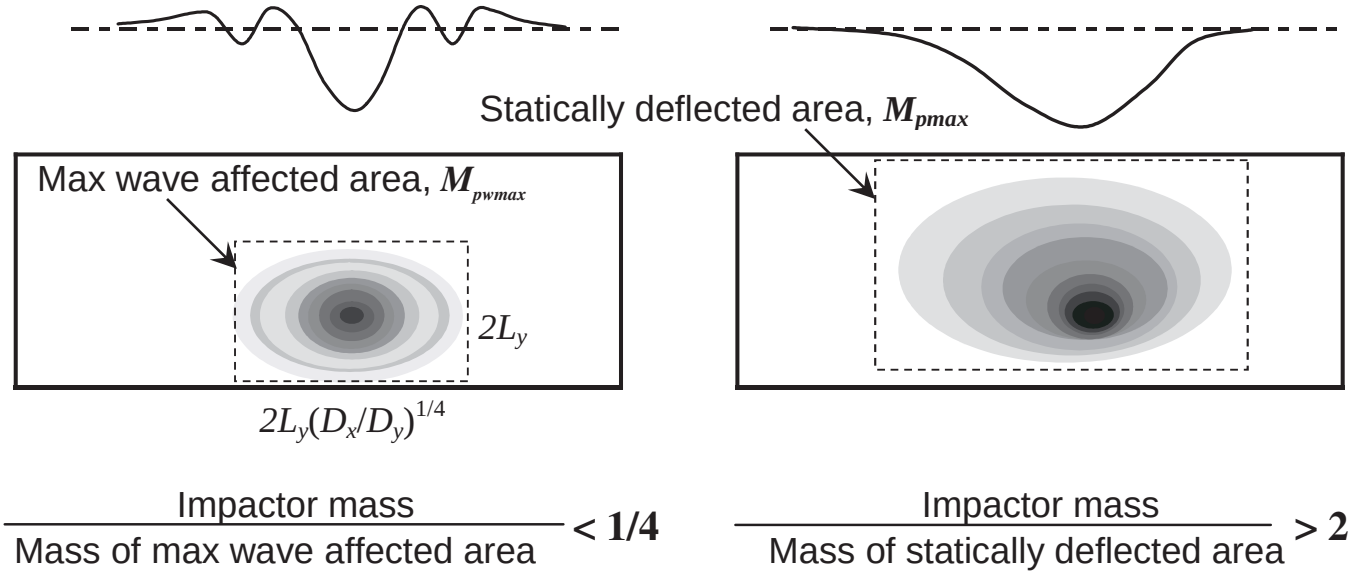
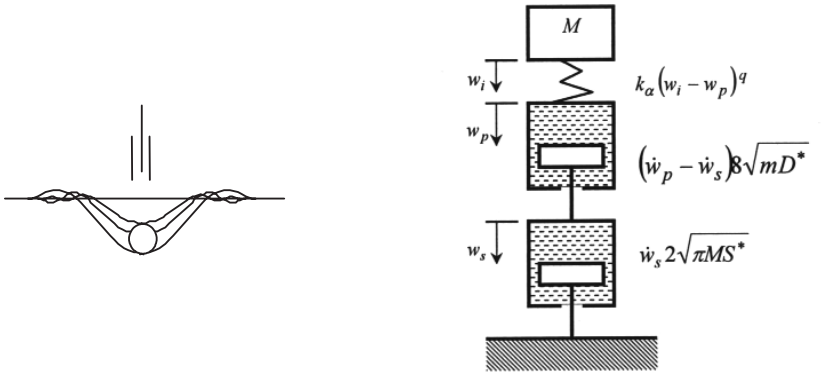


Figure 12. Influence of impactor/plate mass ratio on response type.

https://doi.org/10.1017/S0001924000000385 Published online by Cambridge University Press



V_0	Impact velocity
M	Impactor mass
k_α	Contact stiffness
q	Contact exponent
D^*	Effective plate stiffness
S^*	Shear stiffness
m	Mass per unit area

$$w_p = \frac{1}{8\sqrt{mD^*}} \int F dt$$

Figure 13. Structural model for small mass impact.

between impactor mass, impact time and the mass of the plate, it can be shown that the response type under elastic conditions is *solely dependent on the impactor/plate mass ratios*, Fig. 12, Olsson(2000). For the impacted plate two masses are of particular interest; the mass affected by flexural waves and the mass affected by static deflection.

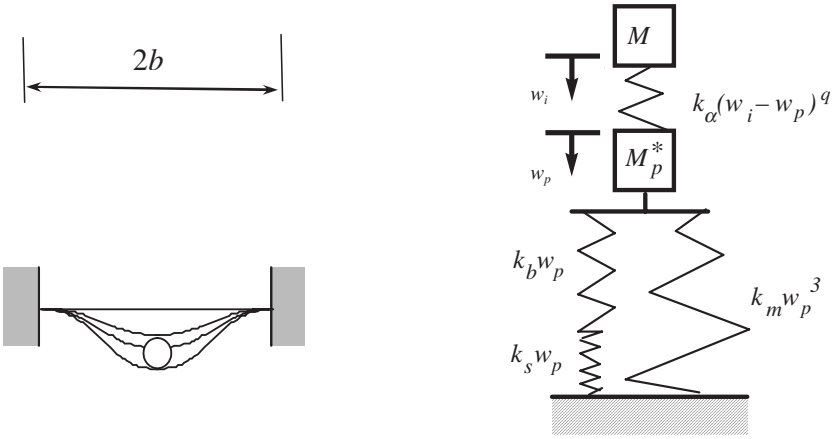
The maximum plate mass M_{pwmax} unaffected by reflected flexural waves is given by a rectangular area centred at the impact location and barely touching any of the plate boundaries. The aspect ratio of this area is given by the ratio of flexural wave speeds $(D_x/D_y)^{1/4}$. For a central impact on a quasi-isotropic square plate M_{pwmax} equals the total mass of the plate, M_p. For impactor masses $M^p < M_{pwmax}/4$ the response is independent of the plate boundary conditions and entirely governed by wave propagation, Olsson(2000). We will call this response type 'small mass impact'.

The maximum plate mass M_{pmax} affected by an impact is defined by the plate mass undergoing any significant deflection due to a static load at the impact centre. For plates with large aspect ratios M_{pmax} is significantly smaller than the total plate mass. The effective dynamic mass M_p^* for a one-degree-of freedom model of the plate is only a fraction of M_{pmax} as the deflection velocity decreases towards supported edges. For a central impact the effective dynamic mass may be estimated from the fundamental vibration frequency ω_1 of the plate, i.e. $M_p^* = k/\omega_1^2$, where k is the flexural stiffness of the plate for a static load at the impact centre. The ratio M_p^*/M_{pmax} typically ranges from 0·15 to 0·25, depending on the boundary conditions of the plate. For impactor masses $M_p > 2M_{pmax} \geq 8M_p^*$ the response will be quasi-static with the deflection and load in phase and having the same relation as under static loading, Swanson(1992). We will call this response 'large mass impact'.

Intermediate mass impactors $1/4 < M/M_p^* < 2$ cause more complex vibrations, where higher frequencies are superimposed on the fundamental vibration of the plate-impactor system. The effect of different impactor/plate mass ratios were clearly demonstrated in a numerical study by Jackson & Poe(1993).

A model for small mass impact response of orthotropic laminates with a Hertzian contact law was presented by Olsson(1992) and validated by extensive experiments. Inelastic contact during impact on isotropic plates was considered by Chattopadhyay and Saxena(1991). Out-of-plane shear of transversely isotropic plates was included in a model by Mittal(1987). This approach was later generalised to orthotropic plates with either Hertzian (monolithic laminates) or linear contact laws (sandwich panels), Olsson(2002). Closed form solutions are obtained for a linear contact law on plates without shear deformation, while other cases require step-wise solution of integral or differential equations. Closed form approximations for the peak impact load were obtained by consideration of asymptotic cases, Olsson(2003a). A schematic representation of the resulting small mass impact model is shown in Fig. 13. Note that the plate is entirely described by the local quantities, $m = \rho h$ and the effective flexural stiffness D^* and shear stiffness S^*, as the response is independent of the plate geometry and boundary conditions. The reader is referred to Olsson(2003a) for a more complete description of the model and its parameters.

Elastic impact models may be used to predict the peak load, which is crucial for prediction of damage intiation. The peak load F_{peak} during small mass impact is approximated by the following expression, Olsson(2003a)



M	Impactor mass
M_p^*	Effective plate mass
k_α	Contact stiffness
k_b	Bending stiffnes ($\sim D/b^2$)
k_s	Shear stiffness
k_m	Membrane stiffness

$k_m = 0,\ k_s = \infty \Rightarrow$
$w_p = F/k_b$

Figure 14. Structural model for large mass impact.

https://doi.org/10.1017/S0001924000000385 Published online by Cambridge University Press

$$1/F_{peak} \approx 1/F_b + 1/F_s + 1/F_c \qquad \text{where}$$

$$F_b = 8V_0\sqrt{mD^*} \qquad F_s = 2V_0\sqrt{\pi MS^*} \qquad F_c = \begin{cases} k_\alpha^{2/5}\left(\frac{5}{4}MV_0^2\right)^{3/5} & \text{for } q = 3/2 \\ V_0\sqrt{Mk_\alpha} & \text{for } q = 1 \end{cases} \qquad \ldots (1)$$

Here q = 3/2 represents a Hertzian contact law, suitable for monolithic plates, and q = 1 a linear contact law, which is a suitable approximation for sandwich panels.

A general model for large-mass and intermediate-mass impact was suggested by Shivakumar *et al*(1985). The model involves the impactor mass, the effective dynamic mass of the plate and a system of springs describing the indentation, bending, shear and membrane stiffness of the plate, Fig. 14. Closed form expressions were given for central impact on circular transversely isotropic plates, but the model may easily be extended to other geometries. Note that the plate must be described by the *global stiffness* in bending, shear and membrane deformation (k_b, k_s and k_m) as the response is dependent on the plate geometry and boundary conditions. It is worth noting that the bending stiffness is proportional to the local bending stiffness D and inversely proportional to the squared span width, $(2b)^2$. The extension to central impact on orthotropic rectangular plates was described by Olsson(2002). Extension to more general geometries is straight forward, although stiffness values may have to be obtained experimentally or by use of numerical methods.

Step-wise numerical methods are required to describe the vibration of the non-linear two degree-of-freedom system. However, for large mass impact ($M >> M_p^*$) the peak force and deflection may be determined from a simple energy balance. The peak load is given by a non-linear equation which equates the initial kinetic energy of the impactor and the total elastic energy at peak load, which may be determined theoretically or by a geometrically nonlinear static FE-analysis, as described by Davies, Hitchings and Wang(2000). If membrane forces are neglected the peak load during large mass impact is given by the expression:

$$1/F_{peak} = 1/F_b + 1/F_s + 1/F_c \qquad \text{where}$$

$$F_b = V_0\sqrt{Mk_b} \quad F_s = V_0\sqrt{Mk_s} \quad F_c = \begin{cases} k_\alpha^{2/5}\left(\frac{5}{4}MV_0^2\right)^{3/5} & \text{for } q = 3/2 \\ V_0\sqrt{Mk_\alpha} & \text{for } q = 1 \end{cases} \qquad \ldots (2)$$

The shear stiffness k_s is a non-constant, fairly complicated function of the load. In most applications $F_b << F_s, F_c$ so that $F_{peak} \approx F_b$.

A simplified two-degree of freedom linear model was suggested by Bucinell, Nuismer & Koury(1991), who neglected membrane and shear effects and used a linearised contact spring based on the peak force for impact on a half-space ($k_b = \infty$). This model provides closed form expressions for the vibration of the system, but yields poor results for intermediate mass impact. The predictions can be drastically improved by a properly linearised contact spring $k_{\alpha L}^*$, based on the *average* contact load during Hertzian impact on the *flexible* plate, Olsson(1993):

$$k_{\alpha L}^* = \tfrac{1}{F_{\max}}\int_0^{F_{\max}} (F/\alpha)\,\mathrm{d}F = \tfrac{3}{4}k_\alpha^{2/3}F_{\max}^{1/3} = \tfrac{3}{4}k_{\alpha L} \qquad \ldots (3)$$

where $k_{\alpha L}$ is a linearised spring at the peak load. The linearised spring $k_{\alpha L}$ is obtained by a brief iterative approach, which considers the peak load during impact on a plate with a *finite* bending stiffness k_b.

To the authors' knowledge published closed form models are only available for flat plates. Models based on summation of contributions from a large number of modes have been presented by Cairns & Lagace(1989) and Sankar(1992) for central impact on plates, where the latter model was limited to simply supported plates. Similar models have also been presented for curved panels. These mode summation models are essentially numerical and allow treatment of both small and large mass impact.

3.4 Criteria for failure initiation

Use of theoretical models for damage prediction relies on appropriate criteria for damage initiation and growth. Locally high contact stresses, transverse shear stresses and back face bending strains cause matrix cracks which act as initiation sites for delamination. Accurate prediction of these initial cracks is complicated but is not a major issue since the cracks are highly localised and have a small influence on the structural response as long as no penetration occurs.

A criterion for damage due to impact-induced through-the-thickness waves was provided by Godwin and Davies(1988). By assuming plane waves the amplitude of the initial compressive strain wave due to an impact at velocity V_0 was given approximately by:

$$\varepsilon = V_0/C_z = V_0/\sqrt{E_z/\rho} \qquad \ldots (4)$$

where C_z is the velocity of through-the-thickness waves. The velocity for damage initiation is given by an appropriate failure strain. The out-of-plane compressive failure of unidirectional carbon/epoxy without lateral support involves matrix shear cracks along the fibres, with failure strains around 3%, but about three times larger for cross-ply laminates, Mespoulet *et al*(2000), and for unidirectional specimens with rigid lateral support, Collings(1974). This effect is explained by the change in failure mechanism from shear cracks along the fibres to shear cracks through the fibres. Pure tensile strains, with failure at 0·5 to 1% strain, occur if the impactor rebounds before the initial compressive stress wave has been reflected back to the impacted face.

Sufficient impact energies result in complete penetration of the laminate, irrespective of the impact velocity. The energy necessary for penetration is consumed in global deformation and (local) penetration energy, which includes energy for delamination and shear out. In carbon fibre plastics the penetration energy is dominated by shear out, Cantwell & Morton(1989). Penetration by a flat-faced impactor of radius R typically involves shearing off fibres along a conical surface A_s. If shearing occurs along the plane of maximum shear stress (45°) the penetration force may then be estimated from:

$$F_{pen} = \tau_{FS}A_s = \sqrt{2}\pi(2R + h)h\tau_{FS} \qquad \ldots (5)$$

where τ_{FS} is the shear strength in the 45° plane and h is the laminate thickness. For carbon reinforced plastics τ_{FS} is around 500MPa. Outside the region controlled by contact stresses delamination growth occurs in mode II under the action of transverse shear stresses. The critical load for axisymmetric growth of a single delamination F_{d1} was derived by Davies & Robinson(1992) while a more thorough derivation for an arbitrary number n of delaminations was provided later by Suemasu & Majima(1996):

$$F_{d1} = F_d(n = 1) \text{ where } F_d = \pi\sqrt{32DG_{IIc}/(n+2)} \qquad \ldots (6)$$

Under small deflections this critical load is independent of the size of the delamination, which grows in an unstable fashion. Geometrically nonlinear (large deflection) effects were later studied by Suemasu & Majima(1998). Clearly the first delamination initiates at the midplane, where the transverse shear stresses have a peak.

https://doi.org/10.1017/S0001924000000385 Published online by Cambridge University Press

Thus the threshold value for delamination growth is given by F_{d1}. Interestingly the threshold load is *independent of delamination size*. The theoretical threshold load is supported by extensive experimental data for various layups, geometries and boundary conditions, Davies & Robinson(1992), Olsson(2001) and Cartie and Irving(2002). Comparisons between the theoretical threshold load and non-linear FE-analysis for various delamination locations were given by Olsson(2001). This paper also showed that the threshold load is independent of boundary conditions for small deflections and how it may be corrected for large deflections by considering the additional load carried by membrane forces, which do not contribute to the delamination growth.

The threshold load has been combined with models for small mass impact to predict delamination onset in intermediate velocity impact by runway debris etc. Olsson(2003a). Comparison with experiments did not indicate significant dynamic effects on the threshold load.

For sandwich panels the delamination load F_{d1} may be used as a lower bound for the actual delamination threshold load, as it neglects the additional local support by the core, Olsson(2002).

3.5 Criteria for impact response with damage growth

Formation of damage during the impact will modify the response more or less extensively. A model for the inelastic impact response of thin laminates with a rigidly supported back face was provided by Yigit & Christoforou(1995). Damage caused by contact stresses, flexural stresses or through-the-thickness waves are usually fairly localised and have a small influence on the flexural response, provided no penetration occurs. In contrast, fibre failure caused by membrane stresses has a significant influence on the response, Davies and Zhang(1995), as shown in Fig. 18. In the case of complete penetration the response will be changed fundamentally, as no more load is transferred to the plate. Delaminations have a profound influence on the flexural stiffness, and consequently affect the impact response whenever flexure is of importance.

Theoretical models for delamination growth during impact are scarce and limited to quasi-static loading (large mass impact). Bostaph & Elber(1983) outlined a membrane-plate model which compared the required and available energy for axisymmetric delamination of circular plates with various numbers and sizes of delaminations. Synthetic load-deflection curves were produced by selecting the curve with the smallest strain energy, and showed good agreement with experiments.

More recently Olsson(2001) modified the model in Fig. 14 to account for delamination growth. This was done by introducing a "mechanical fuse" maximising the load supported by the shear and bending springs to F_d, while the membrane stiffness remains unaffected by delamination. In contrast to the model by Bostaph & Elber(1983) the number of circular delaminations was assumed to

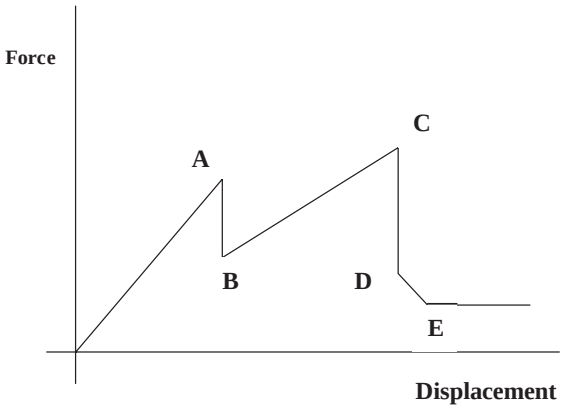


Figure 15. Force history during penetration.

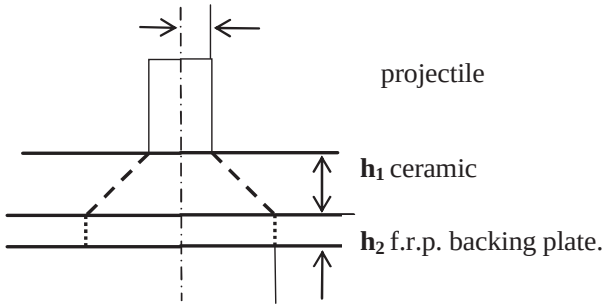


Figure 16. Composite armour system.

reach a "saturated" value n_{max}, which was a predetermined fraction of the total number of interfaces. This fraction was based on the typical ratio (≈30%) between the individual peanut shaped delamination area and the apparently circular area of several superimposed delaminations. Predicted delamination sizes seem to be in fair agreement with experiments up to the point of major fibre fracture, where delamination growth virtually stops.

Interestingly, the prediction of impact damage growth in sandwich panels is substantially easier, as core crushing, face sheet delamination and fibre fracture may be incorporated in the contact model. Thus, the structural model may be kept unchanged, provided the damage is sufficiently local not to affect the global behaviour of the panel. The upper bound of the core crush zone diameter d was derived by Olsson(2002) who also suggested it as a rough upper limit of the delamination size in sandwich panels:

$$d^2 \leq 4F_{peak} / \pi p_{cr} \qquad \ldots \quad (7)$$

where p_{cr} is the crush stress of the core. The predictions were validated by comparison with experiments on a number of different honeycomb cores. It should be noted that the predicted crush zone does not account for elastic relaxation, which may be substantial in certain foam cores.

3.6 Theoretical models for high velocity impact

Considering ballistic velocities first, in spite of the three dimensional nature of the local stress field before perforation, it is useful and enlightening to look at the remarkable success of very simple models used to quantify high velocity impact events and the energy absorbing mechanisms. These mechanisms have been enumerated by Goldsmith *et al*(1995), Zee & Hsieh(1993), and Lee & Sun(1993). Goldsmith used static penetration tests to deduce the contributions from strain energy, matrix and fibre failure, delamination, forming of petals, hole enlargement and friction. The numerical axisymmetrical finite element model of Lee simulated most of these using smeared quasi-isotropic properties; delamination based on matrix cracking and consequent reduction in effective shear stiffness; and finally allowing for a shear plug to form based on achieving a critical strain energy release rate ($G_I + G_{II}$) on the plug surface. The physics then emerged for a force history shown in Fig. 15. (Where **A** corresponds to the formation of matrix cracks, **A-B** is instant delamination, **B-C** is then at reduced stiffness, **C-D** is the plug moving and **D-E** is the plug exit against friction.)

Very simple simulations of this lead to very convenient design tools. For example consider the configuration of an armour system shown in Fig. 16. in which the projectile hits a very hard brittle ceramic plate which then blunts the projectile and causes instant cracking inside a conical volume which spreads the force over a greater area of the plastic backing plate.

https://doi.org/10.1017/S0001924000000385 Published online by Cambridge University Press

In the simpler case of a composite plate, with no ceramic protection, Cantwell & Morton(1989) ignored all mechanisms except the plug 'shear out' cone of assumed half angle 45° (See Equation (5)). Using a fracture energy for the fibre/matrix surface of 37·5kJ/m^2, a very good agreement for the ballistic limit was achieved. This was later confirmed by Taneba *et al*(2003) who then went much further and showed that if the interlaminar shear strength was very low (<30MPa) then delamination becomes the dominant mechanism again, and results in a much greater volume of material affected and more energy absorbed. Returning to the armour configuration in Fig. 16 again, this was modelled successfully by Hetherington *et al*(1991) for a ceramic plate backed by a flexible glass fibre plate. They adopted a much earlier technique by Florence in 1969 which takes the conical volume in the ceramic as fractured when the strong tensile wave is reflected back from the interface, causing delamination at the same time as the GFRP plate receives the impulse. This plate then bulges freely as an unconstrained membrane. The ballistic limit can then be found by assuming all the energy is absorbed by this membrane action. It is given by the expression

$$V^2 = \frac{\varepsilon S h_1 \pi a^2 (1+\psi)}{0{\cdot}91M}$$

where ε and S are the failure strain and stress in the GFRP backing plate, M is the projectile mass, ψ is the mass ratio M_t/M, and M_t is a measure of the target mass excited and given by $M_t = \pi a^2 (\rho_1 h_1 + \rho_2 h_2)$, ρ being the densities of ceramic and backing plate. The radius a of the backing plate affected in Fig. 16 is given by $a = r + 2h_1$, which corresponds to a cone angle of 63°, much shallower than that of 45° assumed by Cantwell for the pure composite. Even with this element of empiricism this approach agreed well with a series of 12 tests. A recent paper by Zaera & Sanchez-Galvet(1998) on a ceramic plate backed by a ductile metal showed the effective angle to be much smaller. However, using the same model, Navarro *et al*(1993) had good predictions for the ballistic limit with a boron nitride ceramic backed by polyethylene fibres in a polyethylene matrix. For a standard NATO projectile of mass 9·55g, a radius of 3·6mm, impacting at 850ms^{-1}, the backing plate deflected by 19mm, which is just acceptable for body armour.

There have been other similar analyses involving an element of empiricism also, such as Zhu *et al*(1992) and Zee *et al*(1993) all of which give credibility to these simple design tools. However the empirical assumptions do need to be calibrated by test, and it does now seem feasible to use numerical 3D analysis (see Section 4) capturing the true physics. Computing power is cheap and the commercial non-linear codes are fairly robust and user-friendly. A numerical model will be expected to simulate the damage, and then find the residual strength also. There have been very few attempts to do this empirically, such as replacing the damage by an equivalent notch, but Jeng *et al*(1992) have produced a simple model based on curve fitting by Caprino(1984) so that the residual strength is given by:

$$\frac{\sigma_r}{\sigma_o} = \{U_0/[½M(V_0^2 - V_r^2)]\}^a$$

where v_R is the residual velocity, and U_o and α are empirical constants which of course have to be found for any individual composite lay-up.

3.7 Theoretical models for residual strength

As mentioned previously, the typical sequence for formation of impact damage consists of matrix cracks, delaminations and finally fibre fracture. Theoretical models for strength after impact have addressed three separate failure mechanisms; 'notch type' failure, sublaminate buckling and delamination growth induced by sublaminate buckling.

'Notch type' models assume in-plane failure caused by stress concentrations resulting from the damage. The simplest approach is to represent the damage by an equivalent hole. This is clearly a reasonable model in tension, where broken fibres may reduce the tensile stiffness almost to zero, Elber(1983) and Sjögren, Krasnikovs and Varna(2001). Obviously, the equivalent hole size should correspond to the region with extensive fibre fracture, as matrix cracks and delaminations have a minor influence on the tensile stiffness. The equivalent hole model has also been applied to compressive failure, Chu(1988) and Hawyes, Curtis and Soutis(2001). In compression the assumption of an equivalent hole is questionable, at least for non-penetrating impacts, as the in-plane stiffness reduction is fairly moderate, Sjögren, Krasnikovs and Varna(2001). The reason is probably the ability of broken fibres to carry limited compressive loads. A non-zero stiffness of the damage may be accounted for by modelling it as a soft inclusion. This was first done for tensile loads by Cairns and Lagace(1990) but the approach has later been applied to compressive loads by Dost, Ilcewicz and Gosse(1988), Xiong *et al*(1995) and Wang(1999). Soft inclusions under biaxial loads were considered by Berbinau, Filiou and Soutis(2001). Most models with soft inclusions use the complex variable method suggested by Lekhnitskii, but a considerably simpler approach is available for quasi-isotropic laminates, Olsson *et al*(2003).

The stiffness of the impact damage is a major issue for soft inclusion models. Cairns and Lagace(1990) modified the tensile stiffness to account for fibre fracture. Wang(1999) used a reduced compressive stiffness based on matching solutions for laminates with degraded properties to experimental data. Dost, Ilcewicz and Gosse(1988), and Xiong *et al*(1995) defined a gradually decreasing compressive modulus from the ratio between applied (apparent) strain and the Euler buckling stress of delaminated strips. However, in contrast to buckling strips, the stress within buckling circular or elliptical sublaminates is neither constant nor uniform, Olsson *et al*(2000). The latter paper also demonstrated that stress concentrations in the surrounding laminate are insignificant, as local stresses increase smoothly towards the edge of a circular buckle. It is worth noting that experimental evidence indicates that the stiffness of an impact damage decreases gradually towards the centre, Elber(1983) and Sjögren, Krasnikovs & Varna(2001). In contrast, all theoretical soft inclusion models assume a damage with uniform stiffness, which is a major limitation as the stress concentrations are strongly dependent on the stiffness gradients. The failure at non-uniform soft inclusions was studied with FE-analysis by Nyman, Bredberg & Schön(2000).

Two major issues in application of 'notch type' models are the failure criterion to be used and the representation of defect size. Dost, Ilcewicz & Gosse(1988) used a conservative maximum strain failure criterion, while all other models involve notch failure criteria which account for the inherent toughness of the material by considering the defect size. A thorough review of notch failure criteria was given by Awerbuch & Madhukar(1985). The most common are generalisations of the point stress criterion and average stress criterion by Whitney & Nuismer(1974). These may be seen as extensions of linear elastic fracture mechanics and assume damage zones much smaller than the defect size. This limitation was overcome in the failure criterion suggested by Soutis & Fleck(1990), which considers the stress carried by the failed material. It should be noted that laminates have entirely different notch sensitivity (toughness) in tension and compression, as a result of differences in the micromechanical failure modes, Olsson *et al*(2003).

Most notch models use an equivalent defect size expressed as a fraction of the projected delamination size, as seen on C-scan. Figure 10 clearly demonstrates that delamination size is not a universal measure for residual strength. It also illustrates the influence of fibre fracture on in-plane compressive failure, as larger span to thickness ratios are known to cause more fibre fracture. A more useful damage measure seems to be the size of the smaller zone with severe fibre fracture, Sjögren, Krasnikovs & Varna(2001).

https://doi.org/10.1017/S0001924000000385 Published online by Cambridge University Press

A model for sequential buckling and compressive failure of an array of sublaminates was suggested by Gottesman *et al*(1994). Observed major delaminations were represented by a number of rectangular delaminations and buckled sublaminates were assumed to carry no load. In spite of these obvious simplifications predictions were in surprising agreement with experiments. The simplification to rectangular sublaminates seems unnecessary, as a closed form serial solution is available for elliptic orthotropic sublaminates, Shivakumar & Whitcomb(1985). Most sublaminates in impact damage are neither symmetric nor balanced and methods to account for this in the buckling analysis have been described by Dost, Ilcewicz & Gosse(1988) and Xiong *et al*(1995).

A theoretical model for growth of elliptical (and circular) delaminations was suggested by Chai & Babcock(1985). A similar model was later successfully applied by Flanagan(1988) to predict delamination growth from an impact damage. The major limitations of these models are neglect of global buckling, the assumption of delamination growth only by change in ellipsis aspect ratio and the inability to separate fracture modes I and II. The lack of mode separation necessitates an assumed mode ratio or conservative calculations based on the lowest critical value, i.e. in mode I.

Most of the failure mechanisms of impacted *sandwich panels* are essentially identical to monolithic laminates, and may be predicted with the models mentioned above. Compression induced dent growth perpendicular to the load is, however, a particular failure mechanism of sandwich panels, and a closed form criterion for this failure was suggested by Olsson(2003b).

All of the presented models show a reasonably good agreement with strength after impact tests, but the predicted failure mechanism is rarely verified by fractographic studies. A comparison between predictions based on soft inclusion 'notch type' failure and onset of delamination growth indicated that delamination growth was the most critical failure mechanism for an impacted 6mm carbon/epoxy laminate, Nyman, Bredberg & Schön(2000). Most predictions are based on a semiempirically determined 'equivalent' size and stiffness of the impact damage. Furthermore, validation is often done on specimens that secure the assumed failure mechanism. Thus 'notch type' failure models have been validated on specimens with antibuckling plates or having such small dimensions that global buckling does not occur. Similarly, models of sublaminate buckling and resulting delamination growth have been validated on laminates with single artificial delaminations or assumed 'typical' circular delaminations in laminates with prevented global buckling, Flanagan(1988) and Cairns, Minguet & Abdallah(1994). Finally, the described theoretical models do not generally consider interaction between different failure mechanisms. In spite of these limitations the available models may provide a qualitative understanding of different parameters affecting strength after impact, provided all competing failure mechanisms are considered separately.

4.0 NUMERICAL SIMULATION

4.1 The software tools

An aim of structural designers is to reduce or eliminate the need for expensive component tests, and therefore be able to predict both the extent of impact damage and the consequent reduction in residual strength. However the nature of composite aerospace structures presents real problems for a theoretical simulation. They can be geometrically complex even though they are composed of thin-walled laminates such as stiffened compression panels for example. There may be very local details giving rise to three-dimensional stress concentrations which can be embryonic sources of failure for laminates with a low through-thickness strength. The strategy for coping with geometrical complexity is of course to use numerical analysis whereby both the geometrical co-ordinates and the structural displacements are represented by discrete values at selected 'nodes'. In the case of the unknown displacements the idea is to choose such small distances between nodes that the assumed 'shape' between them is not crucial. This is the basis of the most commonly used finite element method. The interested reader who is unfamiliar and needs to know can consult the standard texts like Zienkiewicz(1989) or Cook(1981), but we will assume that any engineer has access to the many commercial finite element (FE) codes. Suffice it to say that the standard FE approach is to assume *approximate* displacement functions, then to satisfy the (a) strain-displacement relations *exactly* and likewise the (b) stress-strain law. The equations of equilibrium or motion (c) are then satisfied *approximately* at the many (possibly thousands) of chosen nodes. The accuracy can always be improved by refining the F.E. mesh where necessary.

It is worth noting that in computational fluid dynamics (CFD) the traditional approach has been to use finite *differences* using discrete approximations for the gradients, rather than shape functions, and now fluid/structure interaction problems use a third alternative, the finite *volume* method, where all three relations (a-c) can be satisfied approximately.

A related issue is how to monitor the nodal movements which can be small for structures but large for fluids. Conventionally CFD adopts an *Eulerian* approach where the fluid flows through a fixed grid, and structural analysis uses the *Lagrangian* which follows the small nodal displacements on the original geometry. This can pose problems if the structural displacements are very large as can happen in bird-strike or ballistic and hypervelocity impact. It can also happen at modest impact velocities for composite structures deliberately designed to absorb energy. A relatively new approach is *Smooth Particle Hydrodynamics* (SPH) which allows complete freedom in the disposition of a node, relating any nodal unknowns only to those immediately surrounding it and choosing local curve fitting

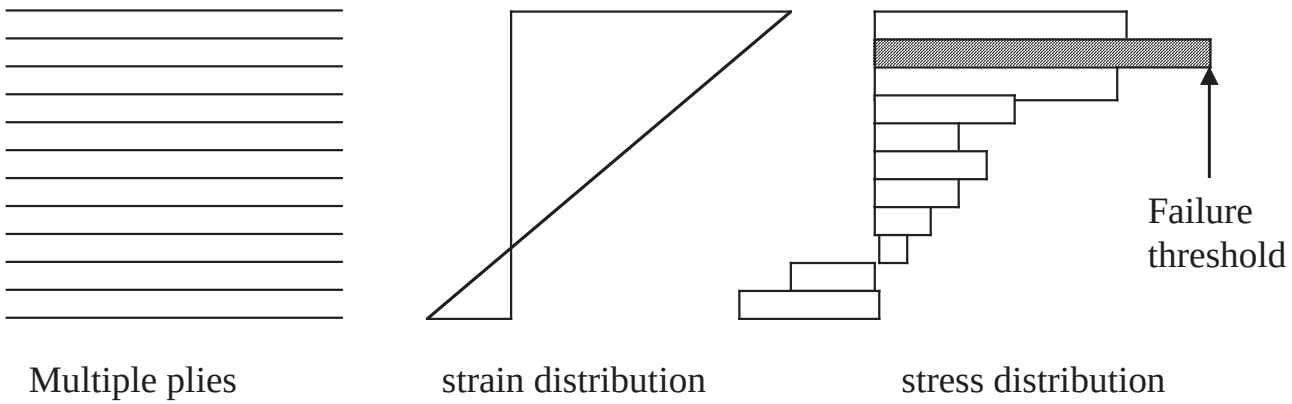


Figure. 17. Strains and stresses in shell structures.

https://doi.org/10.1017/S0001924000000385 Published online by Cambridge University Press

to suit the accuracy required. The method is consequently meshless [see Lucy(1977), Libersky & Petscheck(1993), Morighan(1992) and Groenenboom(1997)] and the conflict between Lagrangian and Eulerian is avoided. SPH codes are being developed to a reasonably mature level by most of the explicit commercial code developers.

Another virtue of numerical analysis is that the true equations of state can be used. The modes of failure, whether in-plane fibre-dominated or through-thickness matrix-dominated, can be complicated and invariably lead to nonlinear behaviour. Likewise any impact on thin-walled structures usually leads to displacements exceeding the local thickness and there will be nonlinear behaviour in allowing for the consequent changes in geometry. Nonlinear FE analysis has not been extensively used as a design tool in the aerospace industry, partly due to the excessive computing time but also because the commercial codes have not been user-friendly or robust and needed experts to use them. This is no longer true. Computing power is becoming extraordinarily cheap and codes are robust and straightforward to use as will be explained shortly.

Firstly we need to discuss the best way to solve the equations of motion for the many displacements **r**(t), that is

$$\mathbf{M}\ddot{\mathbf{r}} + \mathbf{C}\dot{\mathbf{r}} + \mathbf{K}\mathbf{r} = \mathbf{R}(t) \quad \ldots (8)$$

where the mass matrix **M,** the damping matrix **C,** and the stiffness matrix **K,** will be assembled by the code once the elements have been generated. The applied nodal forces **R** can also be generated but in most impact problems will be zero, unless there is interaction with a fluid perhaps.

The *implicit* approach is to represent the velocities $\dot{\mathbf{r}}$ and accelerations $\ddot{\mathbf{r}}$ in terms of the values of **r** at times $t - \Delta t$, t, and $t + \Delta t$, and then solve the many equations from (8) generated by advancing the time t by as many increments as is necessary to simulate the whole impact event. However this solution of the equations becomes very arduous when we recognise that the stiffness matrix **K** is always changing due to the material and geometrical changes.

The alternative *explicit* approach is to rewrite (8) as:

$$\ddot{\mathbf{r}} = \mathbf{M}^{-1}[\mathbf{R}(t) - \mathbf{C}\dot{\mathbf{r}} - \mathbf{K}\mathbf{r}] \quad \ldots (9)$$

and to treat the entire right hand side as known at time t, and then to integrate $\ddot{\mathbf{r}}$ by assuming, say, a linear variation. Further if the mass matrix **M** is lumped into purely diagonal form then no inversion is necessary, and the nonlinear changes in stiffness or damping are simply updated if they are known as functions of $\mathbf{r}(t)$. The attractions of the explicit approach are clear, but the downside is that the integration may not be stable. The time step Δt in integrating forward must be less than the time for a stress wave to cross the stiffest (usually the smallest) finite element (strictly speaking the smallest Eigenperiod of the whole structure.) This critical time step may therefore be extremely small, but this is not important since the whole impact event is of the order of milliseconds, and the time step will need to be small anyway to cope with the complex history of the impact event. There are many commercial codes using this approach, such as DYNA-3D, PAMCRASH, RADIOSS and AUTODYNE etc. and they have long since passed into common usage in the automobile industry for evaluating crashworthiness of prototype designs. However, unlike metallic structures, the problem for laminated composites lies in the complex nature of the material and ply failure leading to permanent damage, which is not amenable to a homogeneous elasto-plastic law as in ductile metals.

The explicit method for solving the equations of motion can also be used with advantage for solving the supposedly 'static' problem of finding the residual strength of the damaged structure. The attraction of using a dynamic code for static loading is that the failure of the damaged structure can result in a dynamic 'snap-through', if the structure is loaded in compression, and the structure jumps from one mode to another. The loading is best applied in increments, and the damping chosen to be critical so that the static solution is reached as quickly as possible. (Davies *et al*(2004))

4.2 Failure

Firstly we consider low velocity impact ($V_0 < 70\text{ms}^{-1}$ from Equation (4)) where the structure has time to respond in flexural and shear waves. In many ways this is the most dangerous form of impact since the impacted surface may recover with no external evidence of damage. Low velocity damage can be a hidden menace, and is often referred to as BVID (barely visible impact damage).There may be in-plane fibre damage and/or interlaminar delamination or debonding between components. We need to consider both in-plane and

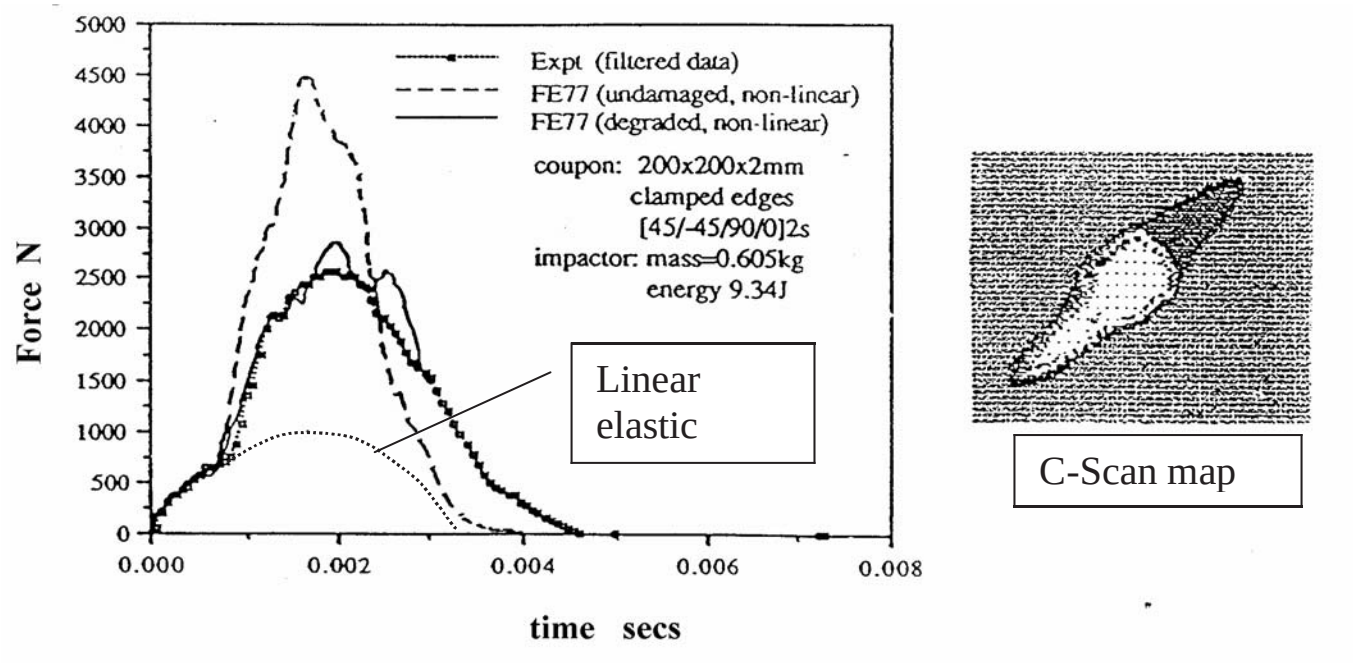


Figure 18. Force histories as predicted and also experimental results.

https://doi.org/10.1017/S0001924000000385 Published online by Cambridge University Press

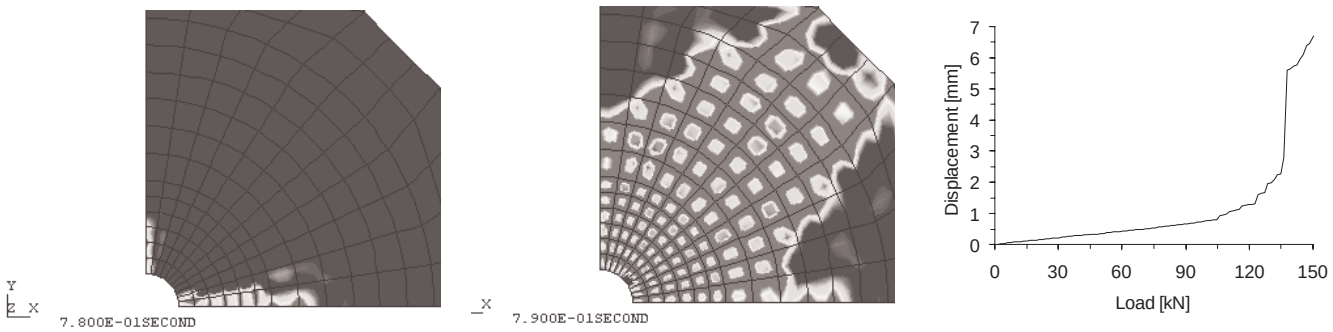


Figure 19. Numerical maps of fibre damage at initiation and failure and a plot of applied load against displacement.

through-thickness mechanisms. Ideally we would use tiny finite elements for every ply and every interface and make no approximations for the three dimensional stress field. However consider a typical aircraft wing skin of 64 ply and a potential damage area of 200 × 200mm. This would need 160 million elements! Moreover the critical timestep would now be of order $\Delta t = t_{ply}/C_z \approx 50$ nanoseconds! It is .therefore reasonable, away from 3D details, to assume that a thin walled structure can be modelled using conventional (but composite) plate and shell elements with linear variation of strain through the thickness. The stresses can still be recovered from the plies' stress/strain laws and they will not have a linear variation, depending on the stacking sequence, as indicated in Fig. 17.

We now consider the failure criteria to be applied to these stress fields, and it is necessary to consider in-plane and through-thickness separately. For example the through-thickness stresses will cause failure in the matrix and lead to delaminations which have a sharp crack front. Finite element models would try to map singular infinite stresses and clearly we need to apply fracture mechanics. The same is not true for in-plane fibre-dominated failures.

4.2.1 In-plane failure

Fibre dominated behaviour has traditionally been evaluated by using unidirectional coupon tests loaded bi-axially and by shear. This is an ongoing research topic which has still not produced a satisfactory envelop in all four quadrants of the tension/compression maps. There are many competing criteria, all involving polynomial interaction curves such as the Tsai-Wu(1971), the Chang-Chang(1987) etc., the latter being a simple quadratic coupling between direct and shear stresses. However the stress at a point is not likely to work for laminates in a complex stress field as it is likely to predict initiation only. Notches (and impact damage) produce stress concentrations and it is known that this does not scale (larger holes are weaker) so some popular approximations to fracture mechanics have been *the point stress criterion* by Nuismer and Whitney(1975) and the *average stress criterion* by Whitney and Nuismer(1974). These need a characteristic length to describe the scale of the stress concentration and unfortunately this length depends on the ply properties and stacking sequence. In fact it is not logical to mimic fracture mechanics when the failure front is diffuse. A more physical approach is the 'ply discount' whereby any ply in any element is degraded as a failure threshold is reached, as implied in Fig. 17. In practice it is found in impact convenient to leave, say, 5% of the stiffness to prevent the small oscillations resulting from the instant and total removal of a ply stiffness. Degrading the stiffness is actually part of a more general continuum damage mechanics (CDM) approach, Ladeveze(1992) [reviewed by Talreja(1994)] and applied to impact by Iannucci *et al*(2001). It is possible to use CDM to model the growth of matrix cracks leading to micro-delamination (Kobayashi(1999)) and then to fibre debonding and finally to fibre failure. The technique can relate all the 'degradation' factors to energy release rates in the ply, and so it bridges the gap between initiation and propagation and it can cope with diffuse crack fronts. This approach has been successfully used in commercial codes by Johnson(2001) and Donadon *et al*(2004) to model impact damage in fabric-reinforced plies. The use of CDM is gradually appearing in commercial codes, although it is computationally expensive and may need a large number of state variables established by basic tests. It

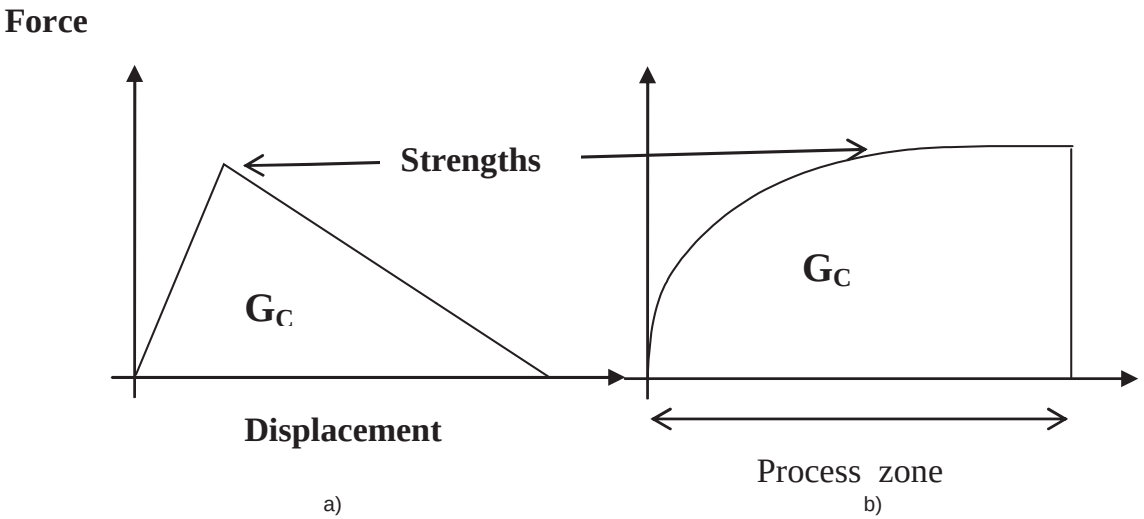


Figure 20. Two forms of interface laws.

https://doi.org/10.1017/S0001924000000385 Published online by Cambridge University Press

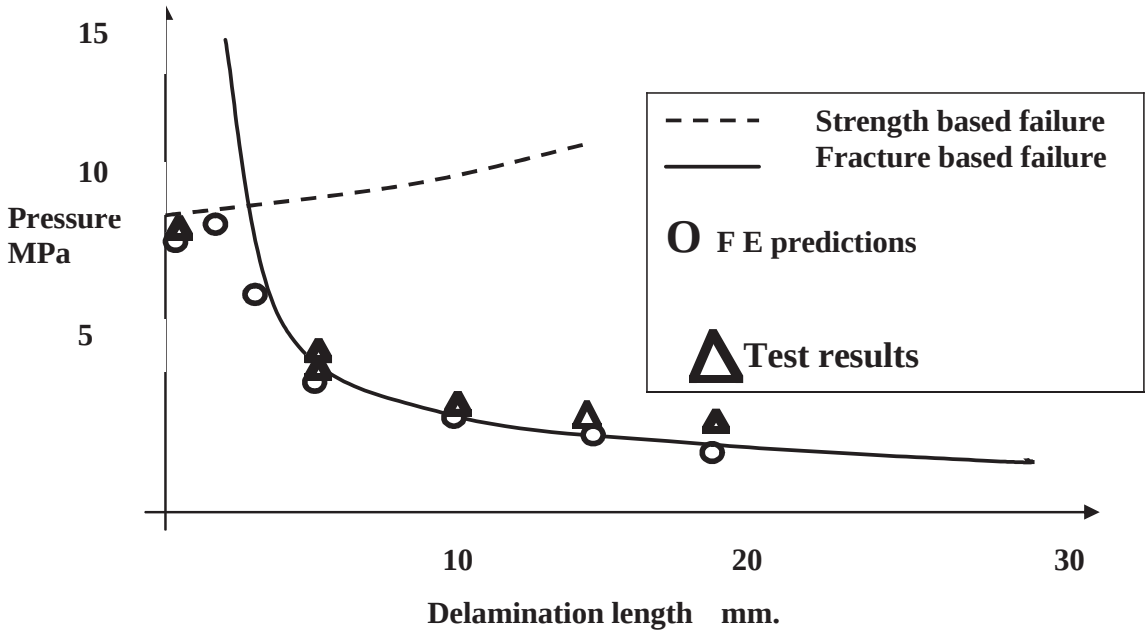


Figure 21. Critical pressure for unstable crack growth as a function of crack length.

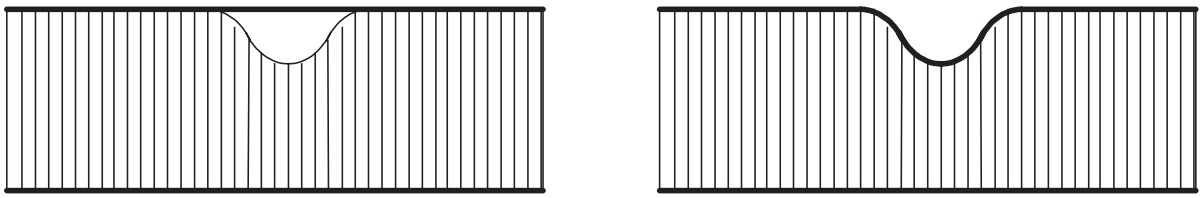
has been found that straight degradation based on strength criteria does reproduce the force history quite well, (Davies *et al*(1995)) and this is a key factor in predicting delamination thresholds. Figure 18 shows the predicted and experimental force histories. The inadequacy of simple elastic theory is clear, but also the need to allow for large deflections where membrane action increases the stiffness enormously. However the consequently large fibre forces are then drastically attenuated by the degradation of the damaged fibres. The C-scan confirms that large scale micro-cracking and delamination has occurred near the back surface. Note that although 2D (degradable) plate elements were used, the loss of energy due to indentation was modelled by using a single element under the impactor site and having the Hertzian indentation law mentioned in Section 2.

The use of some form of degradation means that a finite amount of permanent damage occurs during impact as the stresses rise and fall. However when we use the explicit strategy to simulate the static loading in compression-after-impact tests for residual strength, the question arises of what 'failure' means. In real tests the failure is usually an abrupt loss of structural stiffness and inability to carry the load. We can take the same view numerically. Figure. 19 shows a quarter of a plate with a central circular hole (rather simpler than impact damage) and used in a major collaborative research programme to test the accuracy of the many failure predictive formula in the presence of a strength concentration. It was statically tested to failure, simultaneously under tension (horizontally) and compression (vertically). All of the various criteria, based on the elastic stress field, gave very poor predictions, in this loading case barely a half of the actual failure load in many cases, Davies & Hitchings(2003).The FE simulation produced the damage maps in Fig.19. showing the initiation of fibre damage at the hole edge and then the damage at failure which has extended to most of the plate. The load/displacement curve shows initiation at about 70% of the final failure load. The small residual stiffness after failure is due to the retention of 5% stiffness per ply as mentioned.

4.2.2 Delamination and debonding

Turning to delamination which has a sharp crack front, we really have no alternative but to use fracture mechanics or CDM which uses damage energy release rates. Some codes evaluate the *strain energy release rate* (SERR) around the delamination front and use the known critical value of SERR to propagate. Evaluating the SERR at a point is straightforward by, for example, opening the crack front and evaluating the work done by the nodal forces. However to do this around a complete and moving front needs special software (Nilsson *et al*(1997)) or fitting splines around the front (Roudolff(1998)) This becomes computationally expensive or impossible when a crack jumps to another interface. It is also necessary for the user to invent an initial flaw length somewhere in the structure. One solution to these problems is to use interface elements which can mimic initiation as well as propagation. (Interface elements have also been used by Zou *et al*(2002) but the SERR was evaluated directly in terms of nodal forces and displacements again).

An interface element has zero thickness, and can therefore be inserted in any FE model without disturbing the mesh. It has an



(1) stiff skin, weak bond (2) flexible skin, strong bond

Figure 22. Residual deformation of sandwich panel after impact.

https://doi.org/10.1017/S0001924000000385 Published online by Cambridge University Press

assumed force/displacement law which embraces the physics in either mode I (crack opening) or mode II (shear movements) or a combination of the two. These elements were introduced by Schellekens & de Borst(1993) and have been developed by Crisfield *et al*(1998) using the bilinear force/displacement law shown in Fig. 20(a). This has a rising portion which can mimic the matrix stiffness and has a peak which should match the matrix strength. The falling portion is then adjusted so that the area enclosed is equal to the desired fracture toughness G_{IC} or G_{IIC}. This fixes the baseline distance or 'process zone' which turns out to be a mm. or less. However one disadvantage of this law is that any interface element Gauss point used for sampling may be on the rise but also may be at an equal strength on the fall. This can give rise to oscillations in the deformation history, and has been shown by Crisfield(1998) to be overcome by using elements smaller than the process zone or else sophisticated conjugate gradient iterations with several line searches. A much simpler strategy uses the monotonic curve (an exponential) in Fig. 20(b), where again the initial stiffness, strength and fracture toughness can be chosen to suit.

It has been shown that much bigger elements can now be used, Davies *et al*(2004b). This element has been validated on a large number of benchmarks with theoretical and experimental results, one of which is a circular plate supported around the edge and subjected to a uniform pressure. The shear is a maximum at the edge and decreases linearly to zero at the centre. It can be shown theoretically,

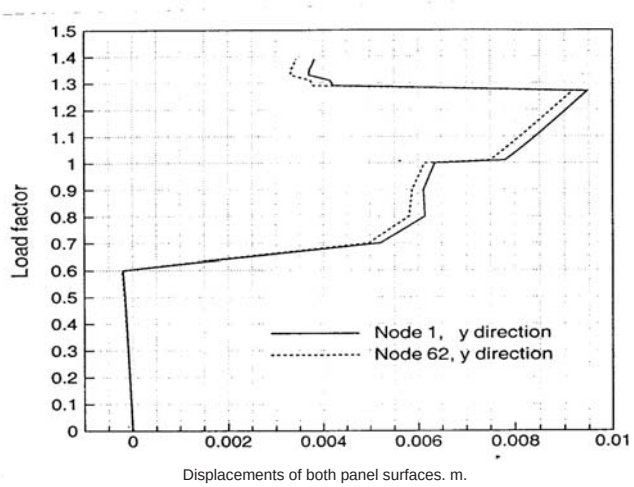


Figure 23. Displacements of panel centre with mid-plane delamination.

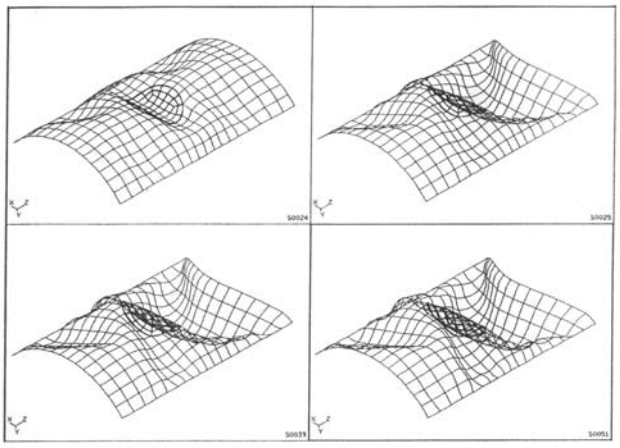


Figure 24. Snap through to antisymmetric mode during CAI loading.

Table 1
Table showing relative contributions of various failure mechanisms in curved panel.

Simulation	Modelling feature	Failure Load kN
Eigenvalue (initial buckling load)	Undamaged panel	209
Incremental	Impact-induced fibre damage only	187
loading using dynamic explicit strategy	Impact-induced fibre delamination also	124
	Further fibre damage during CAI loading	65
	Test value with delamination propagating during CAI loading	51

and by test (Davies(2002)), that a peripheral delamination will propagate inwards in an unstable mode II fashion. Fracture mechanics will predict an infinite critical pressure for zero crack length, but the interface element will automatically start at the strength threshold and switch to the fracture branch at the appropriate point as shown in Fig. 21.

4.2.3 Compression after impact (CAI) strength

Having modelled all forms of impact-induced failure, it is logical to take the damaged structure and numerically subject it to static loading to see how the residual strength has been affected. It is usual to consider the effect on compression behaviour since this is most affected by delamination allowing local macro-buckling and then propagation. There are very few examples in the public domain of predicted impact damage followed by CAI strength evaluation, and here we present just two (Davies *et al*(2004) We look at a sandwich panel, discussed earlier in Section 2.4, and at the two distinctly different forms of damage, illustrated in Fig. 22. In the first case if the skin is stiff, and the skin/core bond is weak, after impact the skin can pull back and leave a crushed core underneath. This poses a hidden problem since at a high enough compression load the unsupported skin can fail by buckling leading to a debonding of the skin from the core. The second case is certainly a visible indentation, and when the panel is loaded in compression the indentation is driven further into the core, the skin bending strains lead to fibre failure, and the indentation propagates catastrophically and transversely across the panel. The failure is dominated by fibre failure and delamination plays no part. The numerical model has to predict the initial impact deformations as well as the CAI failure, involving the skin failure and the core crushing. A full description can be found, Davies *et al*(2004a), including a successful comparison with tests.

A final example is that of a curved panel subjected to a central point impact. The curved panel is much stiffer than the flat, so, for a given energy level, the impact-induced force will be much higher. This leads to much larger areas of delamination and it is expected to result in a significant reduction in residual strength. The use of the explicit dynamic Equations (9) for both the impact event and the CAI static loading is well illustrated in this example. Like a real test we have to define static failure as that load when the structure loses all stiffness. In Fig. 23 we choose to show the displacements of both surfaces at the centre of the panel as the load is applied. If the internal delamination results in a buckle 'opening up' these displacements will be of opposite sign and the crack front will propagate in the weaker mode I. The figure (and the test) shows that the sublaminates buckle together. Initially the shell expands due to Poisson effect but at a load factor of 0·6 (expressed as a ratio of the first eigenvalue) the shell goes unstable and buckles inwards. There then

https://doi.org/10.1017/S0001924000000385 Published online by Cambridge University Press

occurs a series of jumps until at a factor of 1·3 the shell appears to recover. This is deceptive. What actually happens is a sudden mode change shown in Fig. 24. This sort of behaviour can only reliably be captured using the explicit strategy.

The need to model both delamination and fibre damage during impact and during the CAI loading is best summarised in Table 1.

The first eigenvalue gives the initial buckling load as 209kN for the undamaged panel. There would be some post-buckling strength but we are interested in the effect of impact damage. If we allow only fibre damage due to bending strains during impact then the CAI simulation shows failure at 187kN. A bigger reduction to 124kN occurs if we include delamination damage (assumed to occur only at the middle surface). If further fibre damage is allowed during the CAI loading the panel loses all stiffness at a load of 65kN. This represents a 70% reduction from the undamaged buckling load. However the test value, with both fibre damage *and propagation of the delamination occurring*, was 51kN, a reduction of 75%.

4.3 High velocity impact

In previous sections we discussed two cases where the contact pressure was distributed even for high velocity, namely bird strike and hydraulic shock. In both cases the extent of the structure affected can be large and complex, so numerical simulation is the only recourse. Standard commercial codes have long since been used to simulate bird strike on metallic structures. Indeed the aviation certification authorities will accept simulation of, say, a dozen impact cases to identify the single worst case which is then tested.

A numerical code, in addition to coping with complex structures and histories, can also model rate-dependent equations of state that can occur for strain rates in excess of 10^3 per sec. It is known that stiffness and strength can double for ductile metals, but for carbon fibres (Andersen *et al*(1994)) there is little rate effect, whilst for glass fibres there is. For impact damage it is the matrix which can control delamination and here there is limited evidence that the interlaminar shear strength can rise from 70MPa to more than 160MPa at rates in excess of 10^4 per sec.(Chiem *et al*,(1988)). Probably the mode II fracture toughness is of greater importance than the strength, and here the evidence is sparse and inconclusive; some tests show an increase with strain rate, and others a marked decrease at 10^4 per sec. (Sierakowski,(1997)). However in bird-strike for example the main problem could be the gross distortion of the structure and the bird. This puts a strain on the conventional Lagrangian finite element and hydro-codes. Actually a flattened bird simulation does evolve almost stress-free flattened edges where the displacements are a maximum so the contact stresses may still be realistic (Iannucci,(1998)). However if structural deformations are gross then standard commercial codes need to rezone and update the meshes during the impact event. The increasing use of SPH, as mentioned, seems a natural strategy since it is meshless.(Bonet and Kulasegram(2002))

The other need for numerical simulation is for projectile impact at ballistic velocities up to 2,500ms^{-1} and for hypervelocity impact experienced by satellite structures (7-70kms^{-1}) The structural response, for what is usually armour or a bumper shield, can be quite local (less than three or four projectile diameters). Both the structure and the projectile need to be modelled in 3D with a very fine level of discretisation to cope with the gross distortion, and with the phase changes as both bodies experience rapid thermal transport and phase changes from solid through liquid to a gaseous state. The equations of state can nowadays be extremely sophisticated (Andersen(1994)) and beyond the scope of this over-view. Never-the-less the advent of numerical simulation goes back to Mark Wilkins(1978) who as early as 1964 saw the need for a numerical hydro-code at Lawrence Livermore Labs and designed HEMP the fore-runner of PISCES, DYNA-3D and other modern codes. An excellent description of all the various codes available can be found in Zukas(1990). The interested reader is referred to a series of articles in a special journal edition, Ed. Andersen,(2001, 2003) or specifically to Loupias(1997) and Tamura(2003) for impressive demonstrations of the modeling of hyper-velocity events. These events are now amenable to the new SPH codes as was demonstrated in a European programme (Hiermaier *et al*(1999)).

5.0 IMPACT-RESISTANT DESIGNS

Having described the many modes of damage and the tools required to predict them and the compression-after-impact strength, it is of relevance to discuss what can be done to alleviate this weakness of composite structures where the residual compressive strength after low velocity impact may be so low. This section addresses three issues:

- Impact-resistant designs for primary structures.
- Damage tolerance to impact of primary structures.
- Energy-absorbing structures whose residual strength is not an issue.

In comparing competing designs the same realistic incident energy threat should be defined, and here there has been a conflict. The US mil-spec had decided that invisible damage was to be tolerated whilst visible damage had to be inspectable: and so face a decision on whether to repair or replace. A 'visible' indentation of 0·1 inches was chosen which was arbitrary (and illogical since massive impact-induced delamination is possible with indentation almost invisible). Another criterion was a realistic 'threat' of about 140J (another 'arbitrary' 100ftlb) This is unnaturally large, and a more logical stance is to define the threat accurately such as dropped tools or runway debris etc. Thus a 1kg torque wrench dropped from 2m could be 20J, and would be applicable to horizontal upper wing surfaces. On lower surfaces and flaps/controls small-mass runway debris present a real threat of similar energy. Typical threats over a military fuselage , wings and control surfaces range from 15J to 45J.

The damage tolerance of impacted structures is usually measured by the CAI strength, the reason being that delamination is a major consequence and this affects the compressive strength much more than the tensile. Attention has therefore concentrated on stiff-

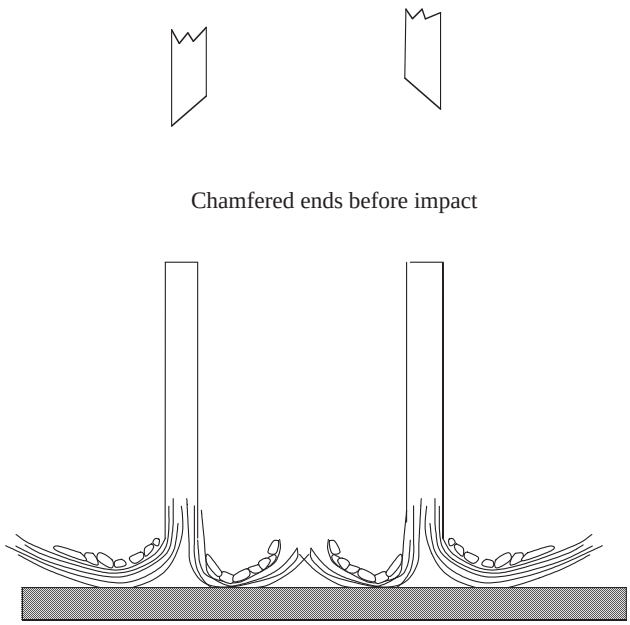


Figure 25. Tube crushing at steady rate and massive release of fibre area.

https://doi.org/10.1017/S0001924000000385 Published online by Cambridge University Press

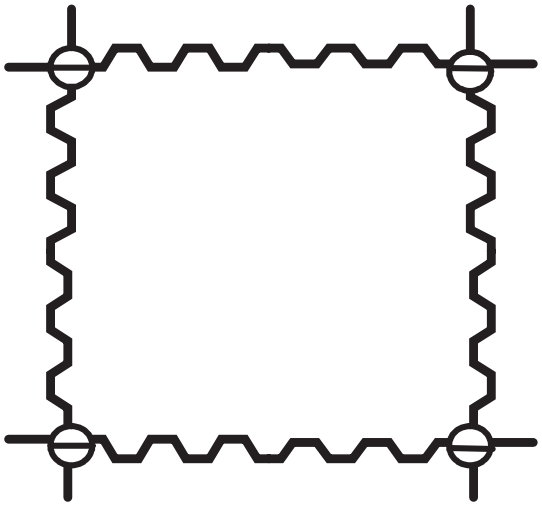


Figure 26. Planform of subfloor beams in a proposed helicopter.

ened compression panels. Wiggenrad *et al*(1999, 2002) took as their starting point Equation (6) which gives the critical force for unstable growth of delamination in terms of $Et^3\ G_{IIC}$. They used this formula (converting force and displacement to energy) as a constraint in a finite strip optimisation code for stiffened panels. The designs were tested and did work, but were a little heavy. Another strategy is to increase the toughness G_{IIC}. Actually most current thermosetting resins do have good fracture toughness values near 600J/m^2 or more, and thermoplastics are much higher, and more expensive. Yet another strategy for increasing toughness artificially is to use Z-pins, a commercial product which drives tiny pins into the laminate prepreg before curing. Again this is expensive and can lower some undamaged properties. A realistic compromise is to use pins as crack stoppers in selected critical areas. Other alternatives such as stitched non-crimp-fabric, woven hybrid combinations using carbon, aramid and glass, are discussed by Greenhalgh & Hiley(2003).The consequence of impact damage for stiffened panels, that is the tolerance or CAI strength, does depend on the detailed design, and the design criteria, and where the panel is impacted. For example an impact between stiffeners can result in a lower force than over a stiffener, but the stiffener is better able to resist the force (Greenhalgh *et al*(1997)). However, this may not always be the case. The shear stresses due to a force on a plate decay like 1/*r* but on a stiffener beam there is very little diffusion into the surrounding skin so the beam shear stays constant all the way to the supporting ribs in a wing box for example. If the impact force is high enough the entire stiffener may debond. However if the main damage is delamination between stiffeners, then on applying compression the sub-laminates may buckle (resisted now by both G_{IC} and G_{IIC}) and cause the delamination to propagate transversely to adjacent stiffeners. This can then cause stiffener debonding, particularly if the panel is loaded into the post-buckled regime. Residual strengths of 60% of the buckling load were found by Greenhalgh(1997) Thus the design of damage tolerant compression panels, without using artificial through-thickness reinforcements, is an exercise in optimising the stiffened panel's proportions.

A final form of damage resistance concerns structures designed deliberately to absorb impact energy, but whose residual strength is of little consequence. Energy absorbing structures have traditionally been made of ductile metals. The trick here is to have a thin-walled structure which resists overall buckling in compression (such as a tube) up to the point at which highly local plastic hinges form. A metal honeycomb is a good example where literally hundreds of hinges form with a half wave length of order the cell size. The USA used such absorbers under the feet of the moon-landers. Unfortunately composites are mainly brittle and were once thought of as poor absorbers. Hull(1982) was the first to show this was untrue. He crushed composite tubes, of various lay-ups, but tailored the end with a chamfer as shown in Fig. 25. The tube then crushed at a more-or-less constant force with massive fibre debonding and matrix cracking. The specific energy absorbed was of order 75kJ/kg for carbon cloth. This compares with 15-30kJ/kg for mild steel and light alloys. This potential has now been recognised and several very efficient energy absorbers have been designed. For example it was recognised that business and general aviation aircraft, made of carbon epoxy, suffered severe vertical retardation in a crash landing, compared with traditional aluminium alloy structures. Kellas(1995) showed that a good energy absorber could be designed in the form of a structural keel beam made as a sandwich beam having two vertical skins made of aramid, and a core made of vertical GFRP tubes filled with foam.

About the ultimate need for a good energy-absorbing sub-floor is the helicopter. Here there is a large mass on the roof, and the passenger cabin should keep its shape in a crash landing. Thus to reduce the fuselage frame loads a good energy absorbing sub-floor is needed. Johnson and Kohlgruber(2000) describe a successful grillage design shown schematically in Fig. 26. The orthogonally intersecting composite beams have the vertically corrugated shear webs to keep the buckling stress high, At the four intersections there are tapered cylindrical-section tubes and all have tailored edges to trigger the fibre -debonding mechanism. Using hybrid composite configurations specific energies greater than 70kJ/kg were achieved.

6.0 CONCLUSIONS

Low velocity impact damage may still be a hidden menace. For composite structural skins up to 8mm. in thickness, and impact incident energies up to 40J, there may be significant damage with little external evidence. The term 'significant' means fibre damage and delamination giving rise to a reduction in compressive residual strength of up to 70%. The actual nature and extent of damage, and the consequent residual strength, depends on many factors including laminate ply and matrix properties, stacking sequence, and overall structural geometry, mass and stiffness. The most important basic material properties are the fibre strains to failure and the matrix fracture toughness. Delamination is controlled by the mode II toughness and the residual compressive strength by both mode II (shear) and mode I (peel). Damage resistance has been improved by better matrix fracture toughness and can also be enhanced by through-thickness reinforcement like weaving, stitching and inserting 'Z-pins.'

Because the whole impact event and aftermath is so complex, it is desirable to be able to predict as much as possible. For basic plates and sandwich panels it has been shown that one or two degree of freedom equivalents can be used to predict the maximum bending strains and impact force. This is sufficient to forecast the *initiation* of damage. For final damage and for modelling more complex structures, such as stiffened panels and shells, the damage can be predicted by modern explicit FE codes and newer developments. The residual strength can also be predicted if the FE model has sufficient fidelity to simulate features like stiffeners, joints and other discontinuities. The credibility of such simulations does need to be established. For bird-strike on leading edges and engine fan-blades, this credibility is approaching that of the well established routines for metallic structures and fan-blades.

For *high (ballistic) velocity* and *hyper (meteorite, space vehicle) velocities* the emphasis is on designing resistance and energy absorption by armour or bumper shields. The damage development at these speeds is extremely local and full three-dimensional models have been successfully validated. The strain-rate material properties need to be known, and in the case of micro-meteorite impact the full equations of state from solid to liquid to gaseous phases.

https://doi.org/10.1017/S0001924000000385 Published online by Cambridge University Press

The benefits of simulating impact at the design stage are clear. Empirical 'knock-down' factors on strength have to be extremely conservative and the weight penalties can be punitive. Structural evaluation and validation by tests is extremely expensive and time consuming.

REFERENCES

ABRATE, S. Impact on laminated composite materials, *Appl Mechs Rev*, 1991, **44,** (4), pp 155-190.

ABRATE, S. Impact on laminated composites: recent advances, *App Mechs Rev*, 1994, **47,** (11), pp 517-554.

ABRATE, S. Localised impact on sandwich structures with laminated facings, *Appl Mechs Rev*, 1997, **50,** (2), pp 69-82.

ABRATE, S. *Impact on Composite Structures*, 1998, Camb Univ Press.

ANDERSEN, C.E., COX, P.A., JOHNSON, G.R. and MAUDLIN P.T. A constitutive formulation for anisotropic materials suitable for wave propagation in computer programmes, *Computational mechanics*, 1994, **15,** pp 201-223.

ANDERSEN, C.E. Hypervelocity impact, Proc of November 2000 symposium at Galveston, 2001, USA, *Int J Impact Engng*, 26.

ANDERSEN, C.E. Hypervelocity impact, proc of 2003 symposium at Noordvijk, 2003, Netherlands, *Int J Impact Engng*, 29.

ASP, L.E., NILSSON, S. and SINGH, S. An experimental investigation of the influence of delamination growth on the residual strength of impacted laminates, *Composites Part A*, 2001, **32,** (9), pp 1229-1235.

AWERBUCH, J. and MADHUKAR, M.S. Notched strength of composite laminates: predictions and experiments — a review, *J Reinf Plastics Composites*, 1985, **4,** (1), pp 3-159.

BERBINAU, P., FILIOU, C. and SOUTIS, C. Stress and failure analysis of composite laminates with an inclusion under multi-axial compression-tension loading, *Appl Compos Mater*, 2001, **8** (5), pp 307-326.

BISHOP, S.M., BRAY, D.J., GREENHALGH., E.G., LAHIFF S. and MILLSON B. The effect of geometry on the impact performance of composite skin-stringer panels, DRA/SMC/CR941005, 1994, DRA, Farnborough.

BONET, J. and KULASEGARAM, S. A simplified approach to enhance the performance of smooth particle hydrodynamics methods, *Appl Maths Communications*, 2002, **126,** pp 133-155.

BOSTAPH, G.M. and ELBER, W. A fracture mechanics analysis for delamination growth during impact in composite plates, in *Advances in Aerospace Structures, Materials and Dynamics, A Symposium on Composites*, 1983, ASME, Boston, pp 133-138.

BUCINELL, R.B, NUISMER, R.J. and KOURY, L. Response of composite plates to quasi-static impact events, in *Composite materials: Fatigue and fracture* (third Vol.), 1991, ASTM STP1110, O'BRIEN T.K., (Ed.) ASTM, Philadelphia, pp 528-549.

CAIRNS, D.S. A simple elasto-plastic contact law for composites, *J Reinf Plast and Composites*, 1991, **10,** (4), pp 423-433.

CAIRNS, D.S. and LAGACE, P.A. Transient response of graphite/epoxy and Kevlar/epoxy laminates subjected to umpact, *AIAA J*, 1989, **27,** (11), pp 1590-1596.

CAIRNS, D.S. and LAGACE, P.A. Residual tensile strength of graphite/epoxy and Kevlar/epoxy laminates with impact damage, *Composite Materials: Testing and Design*, (9th Vol), 1990, ASTM STP 1059, GARBO, S.P., (Ed), ASTM, Philadelphia, pp 48-63.

CAIRNS. D.S., MINGUET, P.J. and ABDALLAH, M.G. Theoretical and experimental response of composite laminates loaded in compression, *Compos Struct*, 1994, **27,** (4), pp 431-437.

CANTWELL, W.J. and MORTON, J. The influence of varying projectile mass on the impact response of CFRP, *Compos Struct*, 1989, **13,** (2), pp 101-114.

CANTWELL, W.J. and MORTON, J. The impact resistance of composite materials: a review, *Composites*, 1991, **22,** (15), pp 347-362.

CAPRINO, G. Residual strength prediction of impacted composite materials, *J Compos Matls*, 1984, **18,** pp 508-518.

CARTIÉ, D.D.R. and IRVING, P.E. Effect of resin and fibre properties on impact and compression after impact of CFRP, *Composites A*, 2002, **33,** (4), pp 483-493.

CHAI, H. and BABCOCK, C.D. Two-dimensional modelling of compressive failure in delaminated laminates, *J Compos Matls*, 1985, **19,** (1), pp. 67-98.

CHANG, F.K. and CHANG, K.Y. A progressive damage model for laminated composites containing stress concentrations, *J Compos Matls*, 1987, **21,** (9), pp 834-855.

CHATTOPADHYAY, S. and SAXENA R. Combined effects of shear deformation and permanent indentation on the impact response of elastic plates, *Int J Solids Struct*, 1991, 27, (13), pp 1739-1745.

CHIEM, C.Y. and LIU, Z.G. Proc IMPACT 87, Impact loading and dynamic behaviour of materials, Ed. Oberursel: DGM Informationsgesellshafft, mbH, 1988, **2,** pp 579-586.

CHRISTOFOROU, A.P., SWANSON, S.R. and BECKWITH, S.W. Lateral impact on composite cylinders, *Composite Materials: Fatigue and Fracture*, 1989, Second volume, ASTM STP 1012, Ed. LAGACE, P.A. ASTM, Philadelphia, pp 373-386.

CHRISTOFOROU, A.P. On the contact of a spherical indenter and a thin composite laminate, *Compos Struct*, 1993, **26,** (1-2) pp 77-82.

CHU, C.S. Simple and generalised strength model for damaged composites, *J Aerospace Engng*, 1988, **1,** (3), pp 131-141.

COLLINGS, T.A. Transverse compressive behaviour of unidirectional carbon fibre reinforced plastics, *Composites*, 1974, **5,** (3), pp 108-116.

COOK, R.D. *Concepts and Applications of Finite Element Analysis*, 1981, 2nd edition, J. Wiley, New York.

CRISFIELD, M.A., MI, Y., DAVIES, G.A.O. and HELLWEG, H-B. Progressive delamination using interface elements, *J Compos Matls*, 1998, **32,** (14) pp 1246-1272.

CURTIS, J., HINTON, M.J., LI, S., REID, S.R. and SODEN, P.D. Damage deformation and residual burst strength of filament-wound composite tubes subject to impact or quasi-static indentation, *Composites B*, 2000, **31,** (5) pp 419-433.

CVITKOVICH, M.K., JACKSON, W.C. Compressive failure mechanisms in composite sandwich structures, *J Am Heli Soc*, 1999, **44,** (4), pp 260-269.

DAVIDSON, B. An experimental investigation of delamination buckling and growth, 31st AIAA/ASME/ASCE/AHS/ASC, Structures, Structural Dynamics and Materials Conf, Long Beach, CA, 1990. Paper AIAA-90-1023, AIAA.

DAVIES, G.A.O. and ROBINSON, P. Predicting failure by debonding/delamination, in Debonding/delamination of composites, 1992, AGARD Conf Proc 530, AGARD, Neuilly sur Seine, France.

DAVIES, G.A.O, ZHANG, X., ZHOU, G. and WATSON, S. Numerical modelling of impact damage, *Composites*, 1994, **25,** (5) pp 342-350.

DAVIES, G.A.O. and ZHANG, X. Impact damage prediction in carbon composite structures, *Int J Impact Eng*, 1995, **6,** (1), pp 149-170.

DAVIES, G.A.O., HITCHINGS, D. and WANG, J. Prediction of threshold impact energy for onset of delamination in quasi-isotropic carbon/epoxy composite laminates under low-velocity impact, *Compos Sci Technol*, 2000, **60,** (1), pp 1-7.

DAVIES, G.A.O, Benchmarks for Composites, 2002, NAFEMS Rep R0084, NEL. East Kilbride.

DAVIES, G.A.O. and HITCHINGS, D. The separate roles of fibre damage and delamination in compression-after-impact strength of composite structures, 5th Euromech solid mechanics conference, 2003, Thessaloniki, Greece.

DAVIES, G.A.O, HITCHINGS, D., BESANT, T., CLARKE, A. and MORGAN, C. Compression after impact strength of composite sandwich panels, *Compos Struct*, 2004a, **63,** (1), pp 1-9.

DAVIES, G.A.O., HITCHINGS, D. and ANKERSEN, J. Predicting delamination in modern aerospace composite structures, to be published in *Compos Sci Technol*, 2004b.

DONADON, M.V., HODGKINSON, J.M., FALZON, B.G. and IANNUCCI, L. Impact damage in composite structures manufactured using resin infusion under flexible tooling (RIFT) process, 2004, ECCM 11, Rhodes, Greece.

DOST, E.F., FINN, S.R., MURPHY, D.P. and HUISKEN, A.B. Impact damage resistance of composite fuselage structure, Part 2, Third NASA Advanced Composites Technology Conf, 1 (Pt2), 1993, pp 759-787.

DOST, E.F., ILCEWICZ, L.B. and GOSSE, J.H. Sublaminate stability based modeling of impact-damaged composite laminates, Proc 3rd Technical Conf Am Soc Composites, Seattle, 1988, pp 354-363.

ELBER, W. Failure mechanics in low-velocity impacts on thin composite plates, 1983, NASA TP 2152, NASA-Langley, VA.

FÄLLSTRÖM, K.E, LINDGREN, L.E., MOLIN, N.E. and WÄHLIN, A. Transient bending waves in anisotropic plates studied by hologram interferometry, *J Exp Mech*, 1989, **29,** (4), pp 409-413.

FERRI, R. AND SANKAR, B.V. Static indentation and low velocity impact tests on sandwich plates, AD, 55, Proc ASME Aerospace Division, ASME, 1997, pp 485-490.

FLANAGAN, G. Two-dimensional delamination growth in composite laminates under compression loading, *Composite Materials: Testing and Design* (8th Vol), 1988, ASTM STP 1206, (Ed) WHITCOMB, J.D., ASTM, Philadelphia, pp 180-190.

GODWIN, W. and DAVIES, G.A.O. Impact behaviour of thermoplastic composites, in *Composite Material Technology*, 1988, BREBBIA, C. (Ed) Springer Verlag.

https://doi.org/10.1017/S0001924000000385 Published online by Cambridge University Press

GOLDSMITH, W., DHARAN, C.H.K. and CHANG, K. Quasi-static and ballistic perforation of carbon fibre composites, *Int J Solids Struct*, 1995, **32,** (1), pp 89-103.

GOTTESMAN, T. *et al* Residual strength of impacted composites: analysis and tests, *J Compos Technol Research*, 1994, **16,** (3), pp 244-255.

GREENHALGH, E.S., BISHOP, S., BRAY, D., HUGHES, D., LAHIFF, S. and MILLSON, B. Characterisation of impact damage in skin-stringer composite structures, *Compos Struct*, 1996, **36,** (3/4), pp 187-207.

GREENHALGH, E.S., SINGH, S. and ROBERTS, D. Impact damage growth and failure of CFRP skin-stringer panels, 1997, ICCM 11, Brisbane.

GREENHALGH, E.S. and SINGH, S. Investigation of the failure mechanisms for delamination growth from embedded defects, 1999, ICCM12, Paris, France.

GREENHALGH, E.S. *et al* The effects of defects on the performance of post-buckled CFRP stringer-stiffened panels, *Composites Part A*, 2003, **34,** (7), pp 623-633.

GREENHALGH, E.S. and HILEY, M. The assessment of novel materials and processes for the impact tolerant design of stiffened composite aerospace structures, *Composites part A*, 2003, **34**, pp 151-161.

GROENENBOOM, P.H.L. Numerical simulation of 2D and 3D hypervelocity impact using the SPH option in PAMCRASH, *Int J Impact Eng*, 1997, **20,** pp 309-323.

HABIB, F.A. A new method for evaluating the residual compression strength of composites after impact, *Compos Struct*, 2001, **53,** (3), pp 309-316.

HAWYES, V.J., CURTIS, P.T. and SOUTIS, C. Effect of impact damage on the compressive response of composite laminates, *Composites Part A*, 2001, **32,** (9), pp. 1263-1270.

HETHERINGTON, J.G. and RAJUGOPALAN, B.P. Investigation into the energy absorbed during ballistic impact of composite armours, *Int J Impact Engng*, 1991, **11,** (1), pp 33-40.

HIERMAIER, S.J., REIDEL, W., HAYHURST, C.J., CLEGG, R.A. and WENTZEL, C.M. Advanced material models for hypervelocity impact simulation, 1999, ESTEC contract 12400/97/NL/PA (SC) Final report.

HULL, D. Energy absorption of composite materials under crash conditions, 1982, ICCM 4, Japan.

HULL, D. and SHI, Y.B. Damage mechanism characterisation in composite damage tolerance investigations, *Compos Struct*, 1993, **23,** (2), pp 99-120.

IANNUCCI, L., DUCHAENE, R., WILLOWS, M. and DEGRIECK, J.A. Failure modes for the analysis of thin woven glass composite structures under impact loadings, *Computers and Structures*, 2001, **79,** (8), pp 785-799.

IANNUCCI, L. Bird strike impact modelling, in Foreign Object Impact and Energy Absorbing Structures, I Mech E conf, 1998, pp 11-29.

JACKSON, W.C. and POE, C.C., The use of impact force as a scale parameter for the impact response of composite laminates, *J Compos Technol Res*, 1993, **15,** (4), pp 282-289.

JENG, S.T., WANG, S.B. and SHEU, L.T. Model for predicting the residual strength of CFRP laminates subject to ballistic impact, *J Reinf Plast Compos*, 1992, **11,** (10), pp 1127-1141.

JOHNSON, A.F. Modelling fibre reinforced composites under impact loads, *Composites A*, 2001, **32,** (9), pp 1197-1206.

JOHNSON, A.F. and KOHLGRUBER, D. Design and performance of energy absorbing subfloor structures in aerospace applications, in Materials and Structures for Energy Absorption, 2000, IMechE Seminar S672, London.

JUPP, J.A. and BRITTON, J.R. Breaking the chain: returning Concorde to service following the Paris accident – July 2000, *Aeronaut J*, July 2003, **107,** (1073), pp 447-458.

KACZMAREK, H. and MAISON, S. Comparative ultrasonic analysis of damage in CFRP under static indentation and low-velocity impact. *Compos Sci and Technol*, 1994, **51,** (1), pp 11-26.

KELLAS, S. An experimental investigation in the energy absorbing performance of composite beam webs for aircraft subfloor applications, 1995, Am Heli Soc, NTS meeting on Rotorcraft Structures, Williamsburg.

KOBAYASHI, S., TAKEDA, N., OGIHARA, S. and KOBAYASHI, A. Damage mechanics analysis of transverse cracking evolution in delaminated CFRP laminates, *J Reinf Plast and Compos*, 1999, **18,** (15), pp 1360-1366.

KONG, C.-W., HONG, C-S. and KIM, C.G. Postbuckling strength of stiffened composite plates with impact damage, *AIAA J*, 2000, **38,** (10), pp 1956-1964.

KRAJCINOVIC, D. Damage mechanics: accomplishments, trends and needs, *Int J Solids Struct*, 2000, **37,** (1-2), pp 267-277.

KUMAR, P. and RAI, B. Delaminations of barely visible impact damage in CFRP laminates, *Compos Struct*, 1993, **23,** (4), pp 313-318.

LADEVEZE, P.A. A damage computational method for composite structures, *Computers and Structures*, 1992, **44,** (2), pp 79-87.

LAGACE, P. *et al*, A preliminary proposition for a test method to measure (impact) damage resistance, *J Reinf Compos and Plast*, 1993, **12,** (5), pp 584-601.

LAINE, R. and FELICI, F. The Giotto dust protective system: testing and numerical analysis of cometry dust impact, *ESA Bulletin*, 1982, **32**.

LEE, S.W.R. and SUN, C.T. A quasi-static penetration model for composite laminates, *J Compos Mater*, 1993, **27,** (3), pp 251-271.

LEVIN, K. Characterization of delamination and fibre fractures in carbon reinforced plastics induced from impact, Mechanical Behaviour of Materials — VI, Kyoto, Proc 6th Int Conf, Ed. JONO, M., Pergamon Press, Oxford, 1991, **1**, pp 519-524.

LIBERSKY, L.D. and PETSCHEK. A.G. *SPH with strength of materials, in Advances in the free Lagrange method*, 1993, TREASE, FRITTS and GROWLEY, (Eds) Springer Verlag, Berlin.

LIU, D. Impact-induced delamination — a view of bending stiffness mismatching, *J Compos Matls*, 1988, **22,** (7), pp 674-692.

LOUPIAS, C., SIBEAUD, J.M. and HEREIL, P.L. Hypervelocity impacts of orbital debris on advanced heat shielding material: comparison of ouranos computations to experimental results, *Int J Impact Eng*, 1997, **20,** (10), pp 545-556.

LUCY, L.B. A numerical approach to the testing of the fission hypothesis, *Astron J*, 1977, **82,** pp 1013-1020.

MELIN, L.G. and SCHÖN. Buckling behaviour and delamination growth in impacted composite specimens under fatigue load: an experimental study, *Compos Sci Technol*, 2001, **61,** (13), pp 1841-1852.

MESPOULET, S., HODGKINSON, J.M., MATTHEWS, F.L., HITCHINGS, D. and ROBINSON, P. Design development and implementation of test methods for through thickness properties of laminated composites, *Plastics, Rubber and Composites*, 2000, **29,** (9), pp 496-502.

MINES, R.A.W., WORRALL, C.M. and GIBSON, A.G. The response of GRP sandwich panels to dropped object impact loading, FRC 90 Fibre Reinforced Composites, 1990, Fourth Int Conf, Proc Inst Mech E, Liverpool, pp 149-155.

MITTAL, R.K. and KHALILI, M.R. Analysis of impact of a moving body on an orthotropic elastic plate, *AIAA J*, 1994, **32,** (4), pp 850-856.

MITTAL, R.K. A simplified analysis of the effect of transverse shear on the response of elastic plates to impact loading, *Int J Solids Struct*, 1987, **23,** (8), pp 1191-1203.

MORIGHAN, J.J. Smooth particle hydrodynamics, *Ann Rev Astrophysics*, 1992, **30,** pp 543-574.

NAVARRO, C., MARTINEZ, M.A. CORTES, R. AND SANCHEZ-GALVEZ, V. Some observations on the normal impact on ceramic faced armours backed by composite plates. Int J Impact Eng, 1993, **13**, (1), *pp 145-156.*

NILSSON, K.F., ASP, L.E. and ALPMAN, J. Delamination and growth at global buckling, First Int Conf on damage and Failure of Interfaces DFI-1, *ed Rossmouth*, Vienna, 1997, pp 193-202.

NILSSON, S. The effect of impact damage on the buckling characteristics of graphite fibre reinforced panels, FFA TN 1994-26, 1994, The Aeron Res Inst of Sweden, Bromma, Sweden.

NUISMER, R.J. and WHITNEY, J.M. Uniaxial failure of composite laminates containing stress concentrations, in *Fracture mechanics of Composites*, 1975, ASTM STP 593.

NYMAN, T., BREDBERG, A. and SCHÖN, J. Equivalent damage and residual strength for impact damaged structures, *J Reinf Plast Compos*, 2000, **19**, (6), pp 428-448.

OLSSON, R. Impact response of orthotropic composite laminates predicted from a one-parameter differential equation, *AIAA J*, 1992, **30,** (6), pp 1587-1596.

OLSSON, R. Impact response of composite laminates — a guide to closed form solutions, FFA TN 1992-33, 1993, The Aeron Res Inst of Sweden, Bromma, Sweden.

OLSSON, R. and MCMANUS, H.L. Improved theory for contact indentation of sandwich panels, *AIAA J*, 1996, **34,** (6), pp 1238-1244.

OLSSON, R. A review of impact experiments at FFA during 1986 to 1998, FFA TN 1999-08, 1999, The Aeron Res Inst of Sweden, Bromma, Sweden.

OLSSON, R. Mass criterion for wave controlled impact response of composite plates, *Composites Part A*, 2000, **31,** (8), pp 879-887 (Correction in *Composites Part A*, **32,** (2) pp 291).

OLSSON, R. Analytical prediction of large mass impact damage in composite laminates, *Composites Part A*, 2001, **32,** (9), pp 1207-1215.

OLSSON, R. Engineering method for prediction of impact response and damage in sandwich panels, *J Sandwich Struct Mater*, 2002, **4**, (1), pp 83-95.

OLSSON, R. Closed form prediction of peak load and delamination onset under small mass impact, *Compos Struct*, 2003a, **59,** (3), pp 340-348.

OLSSON, R. Energy criterion for dent growth in sandwich panels. Proc. 6th

https://doi.org/10.1017/S0001924000000385 Published online by Cambridge University Press

Int Conf on Sandwich Structures, CRC Press, Boca Raton, 2003b, pp 309-409.

OLSSON, R., ASP, L.E., NILSSON, S. and SJÖGREN, A. A review of some key developments in the analysis of the effects of impact upon composite structures, *Composite Structures: Theory and Practice*, 2000, ASTM STP 1383. eds. GRANT, P. and ROUSSEAU, C. (Eds) ASTM, West Conshohocken, pp 12-28.

OLSSON. R., IWARSSON, J., MELIN, L.G., SJÖGREN, A. and SOLTI, J. Experiments and analysis of laminates with artificial damage, *Compos Sci Techn*, 2003, **63,** (2), pp 199-209.

POE, C.C. Simulated impact damage in a thick graphite/epoxy laminate using spherical indenters, *J Reinf Plast Composites*, 1991, **10,** (3), pp 293-307.

PRITCHARD, J.C. and HOGG, P.J. The role of impact damage in post-impact compression testing, *Composites*, 1990, **21,** (6), pp 503-511.

RICHARDSON, M.O.W. and WISHEART, M.J. Review of low velocity impact properties of composite materials, *Composites part A*, 1996, 27, pp 1123-31.

RINAIRD, O. Examination of indentation damage in sandwich panels, 1995, FFA TN 1995-36, Bromma, The Aeron Res Inst of Sweden.

ROBINSON, P. and DAVIES, G.A.O. Impactor mass and specimen geometry effects in low velocity impact of laminated composites, *Int J Impact Engng*, 1992, **12,** (2), pp 189-207.

ROSSEAU, C.Q., BAKER, D.J. and HETHCOCK, J.D. Parametric study of three-stringer panel compression-after-impact strength, *Composite Structures: Theory and Practice*, 2000, ASTM STP 1383. GRANT, P. and ROUSSEAU, C. (Eds), West Conshohocken, ASTM, pp 72-104.

ROUDOLFF, F. Development of delamination models, 1998, ONERA Tech Rep RT 28/7256 DMSE/Y.

ROYLANCE, D. and WANG, S.S. Penetration mechanics of textile structures in flexible reinforced composites, in *Ballistic materials and penetration mechanics*, 1980, Elsevier Sci Pub Co, New York.

SANKAR, B.V. Contact law for transversely isotropic materials, AIAA/ASME/ASCE/AHS 26th Structures, Structural Dynamics and Materials Conference, Orlando FL, Part 1, 1985, pp 516-521.

SANKAR, B.V. Scaling of low-velocity impact for symmetric composite laminates, *J Reinf Plast and Compos*, 1992, **11,** (3), pp 296-309.

SCHELLEKENS, J.C.J. and DE BORST, R. A non-linear finite element approach for the analysis of mode I free-edge delamination in composites, *Int J Solids Struct*, 1993, **30,** (9), pp 1239-1253.

SCHOEPPNER, G.A. and ABRATE, S. Delamination threshold loads for low velocity impact on composite laminates, *Composites A*, 2000, **31,** (9), pp 903-915.

SHIPSHA, A., HALLSTRÖM, S. and ZENKERT, D. Failure mechanisms and modelling of impact damage in sandwich beams — a 2D approach: Part I-Experimental investigation, *J Sandwich Struct Mater*, 2003, **5,** (1), pp 33-51.

SHIVAKUMAR, K.N., ELBER, W. and ILLG, W. Prediction of impact force and duration due to low velocity impact on circular composite laminates, Trans ASME, *J Appl Mech*, 1985, **52,** (3), pp 674-680.

SHIVAKUMAR, K.N. and WHITCOMB, J.D. Buckling of a sublaminate in a quasi-isotropic composite laminate, *J Compos Matls*, 1985, **19,** (1), pp 2-18.

SIERAKOWSKI, R.L. Strain rate effects in composites, *App Mechs Reviews*, 1997, **50,** (11), pt 1, pp 741-761.

SJÖGREN, A., KRASNIKOVS, Y. and VARNA, J. Experimental determination of elastic properties of impact damage in carbon fibre/epoxy laminates, *Composites Part A*, 2001, **32,** (9), pp 1237-1242.

SODEN, P.D. Indentation of composite sandwich beams, *J Strain Anal*, 1996, **31,** (5), pp 353-360.

SOUTIS, C. and FLECK, N. Static compression failure of carbon fibre T800/924C composite plate with a single hole, *J Compos Matls*, 1990, **24,** (5), pp 536-558.

SRINIVASAN, K., JACKSON, W.C., SMITH, B.T. and HINKLEY, J.A. Characterisation of damage modes in impacted thermoset and thermoplastic composites, *J Reinf Plastics and Composites*, 1992, **11,** (10), pp 1111-1126.

STARNES, J.H., RHODES, M.D. and WILLIAMS, J.G. Effect of impact damage and holes on the compressive strength of a graphite/epoxy laminate, Non-destructive evaluation and flaw criticality for composite materials, ASTM STP 696, 1979, pp 145-171.

SUEMASU, H., KETH, S. and MAIER, M. Indentation of spherical head indentors on transversely isotropic composite plates, *J Compos Matls*, 1994, **28,** (17), pp 1723-1739.

SUEMASU, H. and MAJIMA, O. Multiple delaminations and their severity in circular axisymmetric plates subjected to transverse loading, *J Compos Matls*, 1996, **30,** (4), pp 441-453.

SUEMASU, H. and MAJIMA, O. Multiple delaminations and their severity in nonlinear circular plates subjected to concentrated loading, *J Compos Matls*, 1998, **32,** (2), pp 123-140.

SWANSON, S.R. and REZAEE, H.G. Strength loss in composites from lateral contact loads, *Compos Sci and Technol*, 1990, **38,** (1), pp 43-54.

SWANSON, S.R. Limits of quasi-static solutions in impact of composite structures, *Compos Engng*, 1992, **2,** (4), pp 261-267.

TALREJA, R. (Ed) *Damage Mechanics of Composite Materials.*, Composite materials series 9, 1994, Elsevier, Amsterdam.

TAMURA, H., IWAWAKI, M. and SAWAOKA, A.B. Quantatative analysis of debris clouds from duralumin and SiC fibre/aluminum – matrix composite bumpers, *Int J Impact Eng*, 2003, **20,** (10), pp 829-848.

TAN, T.M. and SUN, C.T. Use of statical indentation laws in the impact analysis of laminated composite plates, Trans ASME, *J Appl Mechs*, 1985, **52**, (1), pp 6-12.

TANEBA, Y., AOKI, M., FUJII, K., KARANO, H. and YASUDA, E. Fracture behaviour of CFRPs impacted by a relatively high velocity steel sphere, *Int J Impact Engng*, 2003, **28,** (6), pp 627-642.

TSAI, S.U. and WU, E.M. A general theory of strength for anisotropic materials, *J Compos Matls*, 1971, **5,** pp 58-80.

TSANG, P.H.W. and LAGACE, P.A. Failure mechanisms of impact-damaged sandwich panels under uniaxial compression, AIAA paper 94-1396-CP, AIAA/ASME/ASCE/AHS/ASC 35th Structures, Struct Dyn and Matls Conf, Hilton Head, SC, Pt. 2, 1994, pp 745-754.

TÜRK, M.H. and HOO FATT, M.S. Localized damage response of composite sandwich plates, *Composites Part B*, 1999, **30,** (2), pp 157-165.

WANG, J. Prediction of post-impact compressive strength of composite laminates using an inhomogeneity model, *J Compos Matls*, 1999, **33,** (24), pp 2226-2247.

WARDLE, B.L. and LAGACE, P.A. On the use of quasi-static testing to assess impact damage resistance of composite shell structures, *Mechs Composite Matls and Struct*, 1998, **5,** (1), pp 103-121.

WHITNEY, J.M. and NUISMER, R.J. Stress fracture criteria for laminated composites containing stress concentrations, *J Compos Matls*, 1974, **18,** pp 263-265.

WIGGENRAAD, J.F.M., ZHANG, X. and DAVIES, G.A.O. Impact damage prediction and failure analysis of heavily loaded, blade-stiffened composite wing panels, *Compos Struct*, 1999, **45,** (2), pp 81-103.

WIGGENRAAD, J.F.M., GREENHALGH, E.S. and OLSSON, R. Design and analysis of stiffened composite panels for damage resistance and tolerance, Paper 81208, Fifth World Congr Comput Mech, Vienna, 2002, eds MANG, H.A., RAMMERSTORFER, F.G. and EBERHARDSTEINER, J (Eds).

WILKINS, M.L. Mechanics of penetration and perforation, *Int J Engng Sci*, 1978, **16,** pp 793-807.

WILLIAMSON, J.E. and LAGACE, P.A. Response mechanisms in the impact of graphite/epoxy honeycomb sandwich panels, Proc Am Soc for Composites, 8th Technical Conf, Cleveland, OH, 1993, pp 287-297.

WU, E. AND SHYU, K. Response of composite laminates to contact loads and relationship to low-velocity impact, *J Compos Matls*, 1993, **27,** (15), pp 1443-1464.

WU, E. and YEN, C.S. The contact behaviour between laminated composite plates and rigid spheres, Trans ASME, *J Appl Mechs*, 1994, **61,** (1), pp 60-66.

XIONG, Y, POON, C, STRAZNICKY PV, and VIETINGHOFF H. A prediction method for the compressive strength of impact damaged composite laminates, *Compos Struct*, 1995, **30,** (4), pp 357-367.

YIGIT, A.S. and CHRISTOFOROU, A.P. On the impact between a rigid sphere and a thin composite laminate supported by a rigid substrate, *Compos Struct*, 1995, **30,** (2), pp 169-177.

ZAERA, R. and SANCHEZ-GALVET, V. Analytical modelling of normal and oblique ballistic impact on ceramic/metal lightweight armours, *Int J Impact Engng*, 1998, **21,** (3), pp 133-148.

ZEE, R.H. and HSIEH, C.Y. Energy loss partitioning during ballistic impact of polymer composites, *Polymer Composites*, 1993, **12,** (3), pp 196-202.

ZHANG, X., DAVIES, G.A.O. and HITCHINGS, D. Impact damage with compressive preload and post-impact compression of carbon composite plates, *Int J Impact Engng*, 1999, **22,** pp 485-509.

ZHU, G., GOLDSMITH, W. AND DHARAN, C.K.H. Penetration of laminated Kevlar by projectiles – analytical model. *Int. Jnl. Solids and Structures*, **29**, (4), pp 421- 436, 1992.

ZIENKIEWICZ, O.C. and TAYLOR, R.L. *The Finite Element Method*, 1989, McGraw-Hill.

ZOU, Z., REID, S.R., LI, S. and SODEN, P.D. Application of a delamination model to composite structures, *Compos Struct*, 2002, **56,** (4), pp 375-389.

ZUKAS, J.A. *High Velocity Impact Dynamics*, 1990, Chapter 9, Wiley Interscience, New York.

https://doi.org/10.1017/S0001924000000385 Published online by Cambridge University Press